Article

TRANSPARENT PROCESS

EMBO reports

Retinoblastoma protein promotes uterine epithelial cell cycle arrest and necroptosis for embryo invasion

Shun Akaeda[1], Yasushi Hirota[1,2,*], Yamato Fukui[1], Shizu Aikawa[1], Ryoko Shimizu-Hirota[3], Tetsuaki Kaku[1], Mona Gebril[1], Tomoyuki Hirata[1], Takehiro Hiraoka[1], Mitsunori Matsuo[1], Hirofumi Haraguchi[1], Mayuko Saito-Kanatani[1], Norihiko Takeda[4], Tomoyuki Fujii[1] & Yutaka Osuga[1]

Abstract

Retinoblastoma protein (RB) encoded by *Rb1* is a prominent inducer of cell cycle arrest (CCA). The hormone progesterone (P_4) promotes CCA in the uterine epithelium and previous studies indicated that P_4 activates RB by reducing the phosphorylated, inactive form of RB. Here, we show that embryo implantation is impaired in uterine-specific *Rb1* knockout mice. We observe persistent cell proliferation of the *Rb1*-deficient uterine epithelium until embryo attachment, loss of epithelial necroptosis, and trophoblast phagocytosis, which correlates with subsequent embryo invasion failure, indicating that *Rb1*-induced CCA and necroptosis of uterine epithelium are involved in embryo invasion. Pre-implantation P_4 supplementation is sufficient to restore these defects and embryo invasion. In *Rb1*-deficient uterine epithelial cells, TNFα-primed necroptosis is impaired, which is rescued by the treatment with a CCA inducer thymidine or P_4 through the upregulation of TNF receptor type 2. TNFα is expressed in the luminal epithelium and the embryo at the embryo attachment site. These results provide evidence that uterine *Rb1*-induced CCA is involved in TNFα-primed epithelial necroptosis at the implantation site for successful embryo invasion.

Keywords embryo implantation; progesterone; TNFα signaling; trophoblast phagocytosis; uterine luminal epithelium
Subject Categories Autophagy & Cell Death; Cell Cycle; Development
DOI 10.15252/embr.202050927 | Received 19 May 2020 | Revised 18 November 2020 | Accepted 3 December 2020 | Published online 5 January 2021
EMBO Reports (2021) 22: e50927

Introduction

Infertility is estimated to influence up to 30% of couples worldwide (Inhorn & Patrizio, 2015). The number of infertile patients undergoing *in vitro* fertilization and embryo transfer (IVF-ET) is increasing, and some of these patients repeatedly fail to conceive even after ET using good quality embryos. This pathological condition is called recurrent implantation failure, which becomes a major problem in IVF-ET treatment. Embryo implantation, a series of processes from embryo apposition and attachment to the uterus to embryo invasion into the uterus, is doubtlessly regulated by a precise and intricate molecular interaction between the embryo and uterus (Dey *et al*, 2004; Cha *et al*, 2012; Egashira & Hirota, 2013; Fukui *et al*, 2019; Hirota, 2019). In mice, embryo apposition is followed by intimate adherence of the blastocyst trophectoderm to the luminal epithelium, marking the first discernible sign of implantation from the midnight of day 4 to day 5 morning (day 1 = vaginal plug). This interaction starts when embryonic development is synchronized with uterine preparation to become receptive for implantation. The physiological contact between the blastocyst and the luminal epithelium affects the neighboring stroma, where vascular permeability increases under the control of several factors such as COX2 and VEGF (Matsumoto *et al*, 2002). Blastocyst attachment coincides with increased stromal vascular permeability at the site of the blastocyst called as attachment reaction and can be demarcated by distinct blue bands along the uterus after intravenous injection of Chicago blue dye solution (Das *et al*, 1994). With the implantation process in progress, stromal cells surrounding the implanting embryo undergo decidualization. Decidual growth reaches its peak on day 8 of pregnancy. The luminal epithelium surrounding the implantation sites disappears on day 5 evening, and embryo invasion into the stroma starts from day 5 night to day 6 morning (Matsumoto *et al*, 2018). Our previous observation has indicated that direct contact between embryo and uterine stroma is involved in embryonic cell survival and invasion (Matsumoto *et al*, 2018).

Ovarian steroid hormone progesterone (P_4) governs the entire process of pregnancy, including embryo implantation. By the stage of embryo apposition, P_4 guides the uterus to the receptive state (Dey *et al*, 2004). In mice, pre-ovulatory ovarian estrogen secretion

1 Department of Obstetrics and Gynecology, Graduate School of Medicine, The University of Tokyo, Tokyo, Japan
2 Frontier Outstanding Research for Clinical Empowerment (FORCE), Japan Agency for Medical Research and Development (AMED), Tokyo, Japan
3 Department of Internal Medicine, Center of Preventive Medicine, School of Medicine, Keio University, Tokyo, Japan
4 Center for Molecular Medicine, Jichi Medical University, Shimotuke, Tochigi, Japan
*Corresponding author. Tel: +81 3 3815 5411; Fax: +81 3 3816 2017; E-mail: yhirota-tky@umin.ac.jp

© 2021 The Authors

induces proliferation of the luminal and glandular epithelium during days 1–2 of pregnancy. On day 3, the newly formed corpora luteum produces P_4. By day 4, increasing P_4 causes stromal cell proliferation as well as epithelial cell differentiation detected by epithelial cell cycle arrest (CCA), which we call proliferation–differentiation switching (PDS) in the receptive uterus (Haraguchi *et al*, 2014; Hirota, 2019). PDS regulated by P_4 is associated with the expression of several genes critical for embryo implantation on day 4, followed by attachment of blastocyst to the luminal epithelium from day 4 midnight to day 5 morning. In addition, P_4 acts via the nuclear P_4 receptor (PGR) for transcriptional activation of genes involved in uterine receptivity including PDS and embryo implantation (Lydon *et al*, 1995; Tranguch *et al*, 2007; Haraguchi *et al*, 2014). Thus, P_4-PGR signaling is implicated in the preparation of uterine receptivity and embryo implantation, and uterine epithelial CCA with stromal proliferation is a hallmark of uterine receptivity to the embryo (Dey *et al*, 2004; Cha *et al*, 2012; Haraguchi *et al*, 2014). However, it remains uncertain how P_4-induced epithelial CCA is involved in the process of embryo implantation. The aim of this study is to analyze the underlying mechanisms of embryo implantation by focusing on CCA regulators in the uterus.

A known tumor suppressor retinoblastoma protein (RB) is encoded by *Rb1* gene, and its classical function is to induce CCA by binding and inactivating the transcription factors E2F, repressing the transcription of genes which are required for the S phase (Giacinti & Giordano, 2006; Dick & Rubin, 2013). Therefore, *Rb1* deletion promotes cell cycle progression, which results in loss of cell differentiation. RB acts as a cell cycle suppressor, but it also has the ability to prevent excess action. Unphosphorylated RB (uRB), the active form of RB, has the activity of CCA until a cell is ready to divide. Once cell division is ready, uRB becomes phosphorylated RB (pRB), the inactive form of RB, which releases its binding to E2F factors and loses the function as a cell cycle suppressor (Giacinti & Giordano, 2006; Dick & Rubin, 2013). The previous studies have shown that estrogen increases pRB and promotes cell proliferation in the uterine epithelium, which is suppressed by P_4, indicating that uterine RB controls ovarian hormone-dependent cell proliferation status (Tong & Pollard, 1999; Chen *et al*, 2005). In the present study using female mice with uterine *Rb1* deficiency ($Rb1^{d/d}$ mice), we aimed to investigate the fundamental machinery in which uterine RB and P_4 are involved in embryo implantation through epithelial CCA.

Results

Mice with uterine deletion of Rb1 show subfertility

We first examined the expression of RB in the pre-implantation mouse uterus and found that RB is expressed in the uteri of wild-type (WT) mice from day 1 to day 6 of pregnancy (Fig 1A). In contrast, phosphorylated RB (pRB), the inactive form of RB, is expressed in uterine epithelium on days 2 and 3 but not on day 4 (Fig 1B), suggesting that the suppression of RB activity is lost on day 4. These findings indicate that uterine RB becomes functionally active on day 4 when uterine PDS takes place. To explore the role of uterine *Rb1* in pregnancy, we generated female mice with deletion of *Rb1* in the uterus ($Rb1^{d/d}$ mice) by crossing *Rb1*-loxP mice with *Pgr-Cre* mice. We next confirmed that RB expression is efficiently deleted in $Rb1^{d/d}$ uteri (Fig 1C). In contrast to the uterus, RB expression is normal in the granulosa and lutein cells of $Rb1^{d/d}$ ovary (Fig 1D). $Rb1^{d/d}$ mice and their littermate controls ($Rb1^{f/f}$ mice) were mated with WT fertile male mice. We found that the number of pups delivered by $Rb1^{d/d}$ dams is reduced (Fig 1E), suggesting that uterine *Rb1* is critical for successful pregnancy. Based on these results, we next focused on the role of uterine *Rb1* in embryo implantation.

$Rb1^{d/d}$ mice show normal ovulation and pre-implantation embryo development, but cell cycle arrest of luminal epithelium and embryo implantation are impaired

We examined ovulation and fertilization in $Rb1^{d/d}$ mice by flushing eggs and/or embryos on day 2 of pregnancy and found that both processes are normal (Fig 2A and B). We also confirmed normal development of pre-implantation embryos and their timely transport from the oviduct into uterine lumens of $Rb1^{d/d}$ mice by recording the number of blastocysts retrieved by flushing on day 4 of pregnancy (Fig 2C), suggesting that pre-implantation ovarian and oviductal functions are normal in $Rb1^{d/d}$ mice. PDS, luminal epithelial CCA, and stromal proliferation, in the uterus on day 4 morning, are hallmarks of uterine receptivity in embryo implantation (Haraguchi *et al*, 2014; Hirota, 2019). Immunostaining of Ki67, a marker of cell cycle progression, revealed that $Rb1^{d/d}$ mice have increased numbers of proliferating cells in the luminal epithelium on day 4 compared with $Rb1^{f/f}$ mice (Fig 2D and E), suggesting impaired epithelial CCA and uterine receptivity in $Rb1^{d/d}$ mice. We found that the number of distinct implantation sites in $Rb1^{d/d}$ mice is comparable to $Rb1^{f/f}$ mice on day 5 morning (Fig 2F and G). By hematoxylin and eosin (H&E) staining, we confirm that embryo attachment occurs normally in $Rb1^{d/d}$ mice (Fig EV1A), and the expression of COX2, a marker of attachment reaction, is also normal (Fig EV1B). LIF, a key inducer of embryo attachment, activates and phosphorylates STAT3. The expression of *Lif* mRNA and phosphorylated STAT3 (pSTAT3) protein was also normal in $Rb1^{d/d}$ mice (Fig EV1C and D), suggesting that embryo attachment is normal in $Rb1^{d/d}$ mice. To determine whether the implantation process after embryo attachment is normal in $Rb1^{d/d}$ mice, we counted the number of implantation sites in $Rb1^{d/d}$ and $Rb1^{f/f}$ mice on day 8 of pregnancy. The number of implantation sites remained comparable between the two groups on day 8, but increased resorption sites with internal bleeding were observed only in implantation sites of $Rb1^{d/d}$ mice, not in those of $Rb1^{f/f}$ mice on day 8 (Fig 2H and I). By H&E staining, we confirmed that embryos are completely degraded in $Rb1^{d/d}$ mice on day 8 of pregnancy (Fig 2J), suggesting that embryo implantation fails after normal embryo attachment in $Rb1^{d/d}$ mice. Concomitantly with embryo resorption, the weight of implantation sites decreased in $Rb1^{d/d}$ mice (Fig 2K). The mRNA expression of decidualization markers *Cox2* and *Bmp2* was comparable between $Rb1^{d/d}$ and $Rb1^{f/f}$ mice on day 8 (Fig 2L and M), suggesting that degradation of embryos in $Rb1^{d/d}$ mice is not due to decidualization failure.

Intact alignment of luminal epithelium surrounding the embryo and impaired trophoblast phagocytosis are associated with embryo invasion failure in $Rb1^{d/d}$ mice

We next assessed embryo invasion by investigating the elimination of luminal epithelium alignment and trophoblast invasion at the

 © 2021 The Authors

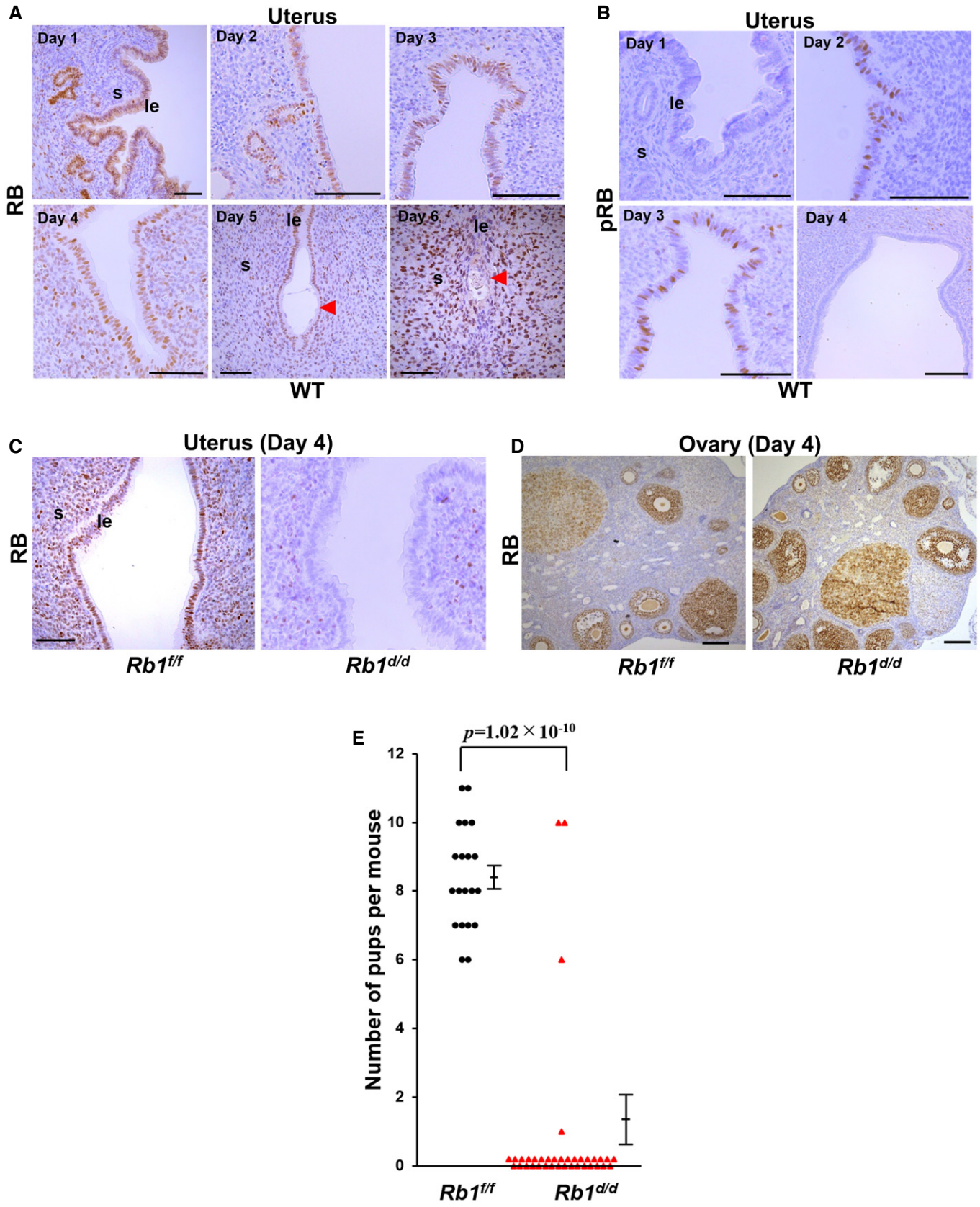
A
Uterus
Day 1
Day 2
Day 3
Day 4
Day 5
Day 6
s
le
RB
WT
B
Uterus
Day 1
Day 2
Day 3
Day 4
le
s
pRB
WT
C
Uterus (Day 4)
s
le
RB
Rb1f/f
Rb1d/d
D
Ovary (Day 4)
RB
Rb1f/f
Rb1d/d
E
p=1.02 × 10-10
Number of pups per mouse
0
2
4
6
8
10
12
Rb1f/f
Rb1d/d

Figure 1.

Figure 1. Mice with uterine deletion of *Rb1* show subfertility.

A Rb1 protein (RB) was expressed in uterine luminal epithelium and stroma during early pregnancy in mice. Scale bar = 100 μm; arrowhead, embryo.
B Phosphorylated RB (pRB) protein, the inactive form of RB, was expressed in the luminal epithelium on days 2 and 3 of pregnancy. Scale bar = 100 μm.
C RB was efficiently deleted in the uterus of mice with uterine deletion of *Rb1* ($Rb1^{d/d}$ mice) on day 4 of pregnancy. Scale bar = 100 μm.
D RB expression was normal in the ovary of $Rb1^{d/d}$ mice on day 4 of pregnancy. Scale bar = 100 μm.
E The number of new-born pups was decreased in $Rb1^{d/d}$ dams (n = 37 different dams) compared with their littermate controls ($Rb1^{f/f}$ mice, n = 20 different dams) (mean ± SEM, Student's t-test).

Data information: le, luminal epithelium; s, stroma.

implantation site, which is a critical process for embryo invasion (Matsumoto *et al*, 2018). Cytokeratin 8 (CK8), a marker of epithelial cell lineage, was used to identify the uterine epithelium and trophoblast. $Rb1^{f/f}$ mice demonstrated that luminal epithelial alignment is collapsed and eliminated around the implantation site at 20:00 h on day 5, and the area of trophoblast invasion is expanded at 09:00 h on day 6 (Fig 3A). In contrast, $Rb1^{d/d}$ mice show that alignment of the luminal epithelium is persistent without trophoblast invasion at implantation sites at 20:00 h on day 5, and embryo invasion is compromised and limited at 09:00 h on day 6 (Fig 3A). Transmission electron microscopic analyses (TEM) of embryo–uterine interface at 20:00 h on day 5 demonstrated direct contact between trophoblast and stroma at the area of eliminated luminal epithelium in $Rb1^{f/f}$ mice but not in $Rb1^{d/d}$ mice (Fig 3B), suggesting the role of uterine *Rb1* in trophoblast invasion by eliminating luminal epithelium alignment. These findings indicate that intact alignment of luminal epithelium is associated with embryo invasion failure in $Rb1^{d/d}$ mice. Surprisingly, TEM revealed that the cytoplasm of the luminal epithelium with lipid droplets is trimmed and engulfed by trophoblast cells, and its nucleus is not apparently condensed in control mice (Figs 3C and D), suggesting luminal epithelium elimination at implantation sites is due to trophoblast phagocytosis of the luminal epithelium. Dying cells exude phosphatidylserine (PS) in their outer membranes to enable phagocytic cell detection. To evaluate the presentation of PS in the outer cellular membrane of the luminal epithelium at the implantation site, we performed immunofluorescence of MFG-E8 as a marker of PS in the outer membrane. Indeed, we found that MFG-E8 is not present in the outer membrane of $Rb1^{d/d}$ mice but in that of $Rb1^{f/f}$ mice immediately before embryo invasion (Fig 3E). Cytoplasmic lipid droplets, which are present specifically in programmed cell death such as apoptosis and necroptosis (Boren & Brindle, 2012; Yamanaka *et al*, 2014; Zhu *et al*, 2016), were not observed in the luminal epithelium of $Rb1^{f/f}$ mice on day 4, but were apparent on day 5 evening (Fig 3D). In contrast, this phenomenon was not detected in the epithelium of $Rb1^{d/d}$ mice on day 5 evening (Fig 3B), indicating that cytoplasmic lipid droplets are characteristic findings of programmed cell death of the luminal epithelium during normal embryo invasion.

Pre-implantation P_4 supplementation is sufficient to normalize epithelial CCA and embryo invasion in $Rb1^{d/d}$ mice

To confirm whether ovarian functions of $Rb1^{d/d}$ mice other than ovulation and fertilization are normal, we first examined the expression of a key steroidogenic enzyme *Hsd3b1* mRNA in the ovary and found that the levels of *Hsd3b1* mRNA are comparable between $Rb1^{d/d}$ and $Rb1^{f/f}$ ovaries on day 4 of pregnancy (Fig EV2A). We next examined the circulating levels of estradiol-17β (E_2) and P_4 during embryo implantation, and found that serum levels of E_2 and P_4 are comparable between $Rb1^{d/d}$ and $Rb1^{f/f}$ mice on days 4 and 6 (Fig 4A and B), suggesting that ovarian functions are normal in $Rb1^{d/d}$ mice in early pregnancy and the reproductive phenotypes of $Rb1^{d/d}$ mice are due to uterine *Rb1* deletion. Since E_2 and P_4 act via nuclear receptors estrogen receptor α (ERα) and PGR, respectively, and we next investigated uterine ERα and PGR by immunostaining. The expression pattern of ERα and PGR in $Rb1^{d/d}$ uteri looked comparable to $Rb1^{f/f}$ ones (Fig EV2B and C). The expression of Forkhead Box O1 (FOXO1), which interacts with P_4-PGR signaling and regulates embryo implantation (Vasquez *et al*, 2018), was also comparable between these mouse uteri (Fig EV2D). In addition, uterine mRNA levels of E_2- and P_4- responsive genes, all of which were reported previously (Tranguch *et al*, 2007; Franco *et al*, 2012; Wetendorf *et al*, 2017), were comparable between $Rb1^{d/d}$ and $Rb1^{f/f}$ uteri on day 4 of pregnancy (Fig EV3A and B), suggesting uterine P_4-PGR signaling is normal. Since we have shown that epithelial CCA in the receptive uterus is induced by P_4, we tried to examine whether exogenous supplementation of P_4 in $Rb1^{d/d}$ mice recovers abnormal epithelial cell cycle status on day 4 morning. As expected, the injection of P_4 (2 mg/day/mouse) on days 2 and 3 normalized epithelial cell cycle status in $Rb1^{d/d}$ mice on day 4 (Fig 4C–E). The administration of exogenous P_4 on days 2 and 3 lead to the circulating P_4 levels on day 4 of pregnancy as highly as those in $Rb1^{f/f}$ and $Rb1^{d/d}$ mice without P_4 treatment on day 6 (Fig 4B). Daily P_4 administration from day 2 to day 7 throughout the implantation period in $Rb1^{d/d}$ mice recovered resorption on day 8, suggesting P_4 normalizes embryo invasion in $Rb1^{d/d}$ mice (Fig 4F and G; Group 1). Next, we examined whether the timing of P_4 supplementation is critical for recovering embryo invasion in $Rb1^{d/d}$ mice. In $Rb1^{d/d}$ mice on day 8, the resorption rate in mice with post-implantation P_4 treatment on days 5–7 was as high as $Rb1^{d/d}$ mice without P_4 treatment (Fig 4F and G; Group 3). In contrast, pre-implantation P_4 treatment on days 2 and 3 completely rescued the implantation sites of $Rb1^{d/d}$ mice (Fig 4F and G; Group 2). More importantly, pre-implantation P_4 treatment on days 2 and 3 recovered subfertility of $Rb1^{d/d}$ mice completely (Fig 4H). This pre-implantation P_4 treatment did not increase blood P_4 levels on day 6 (Fig 4B), suggesting that the pre-implantation P_4 administration influences the uterus until embryo attachment. These findings indicate that pre-implantation P_4 supplementation is sufficient not only to normalize epithelial CCA but to recover embryo invasion and full-term pregnancy in $Rb1^{d/d}$ mice.

TNFα-related necroptosis of the luminal epithelium at the implantation site is impaired in $Rb1^{d/d}$ mice

Since our recent study has revealed that apoptosis is not a key mechanism for the initial step of the luminal epithelium

 © 2021 The Authors

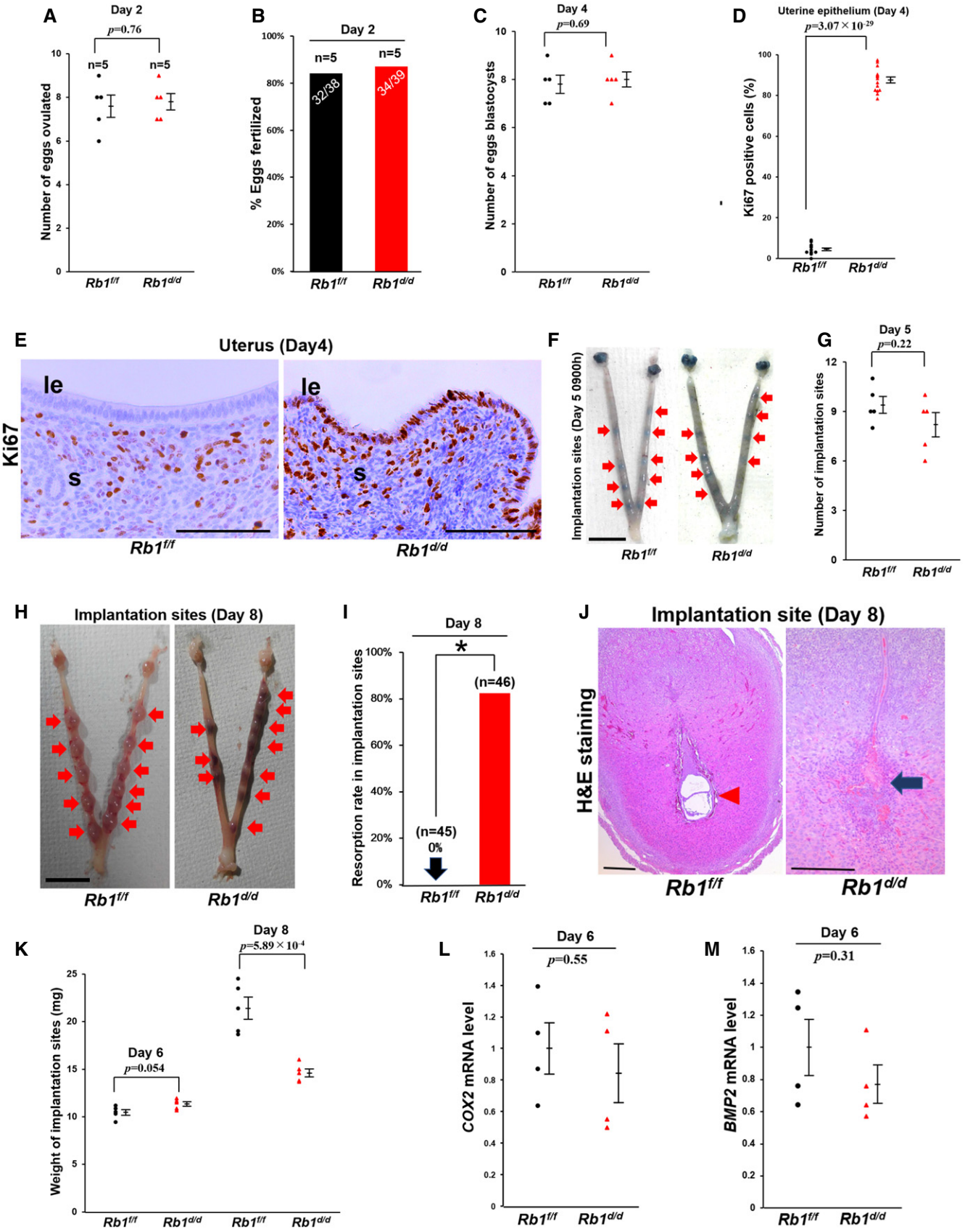

Figure 2.

© 2021 The Authors

Figure 2. *Rb1*$^{d/d}$ mice show impaired pre-implantation epithelial cell cycle arrest and implantation failure.

A–C Ovulation, fertilization, and development of pre-implantation embryos were normal in *Rb1*$^{d/d}$ mice (A and C, mean ± SEM, Student's *t*-test; $n = 5$ mice for each group; B, Fisher's exact test; $n = 5$ mice for each group).

D, E Number of Ki67-positive cells on day 4 in uterine epithelium of *Rb1*$^{d/d}$ mice was higher than that of *Rb1*$^{f/f}$ mice (mean ± SEM, Student's *t*-test; $n = 5$ mice for each group). Scale bar = 100 μm; le, luminal epithelium; s, stroma.

F, G Embryo attachment occurred normally in *Rb1*$^{d/d}$ mice at 09:00 h on day 5 (mean ± SEM, Student's *t*-test; $n = 5$ mice for each group). Arrow, implantation site; scale bar = 1 cm.

H, I *Rb1*$^{d/d}$ mice showed higher rate of embryo resorption on day 8 (*$P < 0.05$; Fisher's exact test; $n = 45$ implantation sites for *Rb1*$^{f/f}$ mice and $n = 46$ implantation sites for *Rb1*$^{d/d}$ mice). Arrow, implantation site; scale bar = 1 cm.

J H&E staining showed embryo resorption in *Rb1*$^{d/d}$ mice on day 8 of pregnancy. Scale bar = 200 μm; arrowhead, embryo; arrow, broken embryo with blood cell infiltration.

K Weight of implantation site was comparable between *Rb1*$^{f/f}$ and *Rb1*$^{d/d}$ mice on day 6, but reduced on day 8 in *Rb1*$^{d/d}$ mice compared with *Rb1*$^{f/f}$ mice (mean ± SEM, Student's *t*-test; $n = 6$ mice for each group).

L, M Expression of *Cox2* and *Bmp2*, markers of decidualization, was comparable in between *Rb1*$^{d/d}$ and *Rb1*$^{f/f}$ mice at 09:00 h on day 6 in implantation sites (mean ± SEM, Student's *t*-test; $n = 4$ mice for each group).

Data information: le, luminal epithelium; s, stroma; tr, trophoblast; n, nucleus.

disappearance around the embryo (Matsumoto *et al*, 2018), we hypothesized that the major machinery of luminal epithelium elimination is necroptosis, another type of programmed cell death. To clarify our hypothesis, we performed immunofluorescence of pRIP3, a marker of necroptosis, and found that pRIP3 is expressed in the membrane of *Rb1*$^{f/f}$ mice but not in that of *Rb1*$^{d/d}$ mice (Fig 5A). We also found that TNFα stimulated phosphorylation of MLKL, a critical signaling pathway of necroptosis, in primary mouse uterine epithelial cells (Fig 5B). Furthermore, uterine expression levels of TNFα was increased after embryo attachment in control mice (*Rb1*$^{f/f}$ mice) (Fig 5C), and both embryo and uterus at the implantation site produced TNFα in *Rb1*$^{d/d}$ mice as intensely as in *Rb1*$^{f/f}$ mice (Fig 5D), suggesting that TNFα-induced necroptosis is compromised by the mechanism which is downstream of TNFα signaling in *Rb1*$^{d/d}$ mice.

P_4-induced CCA of uterine epithelial cells contributes to susceptibility to TNFα and TNFα-primed necroptosis through TNF receptor type 2

PS presentation in the outer membrane is associated with necroptosis (Guo *et al*, 2009; Ehrhardt *et al*, 2013; Zargarian *et al*, 2017). We evaluated the effects of TNFα on necroptosis of primary mouse uterine epithelial cells obtained from *Rb1*$^{f/f}$ and *Rb1*$^{d/d}$ mice. The expression of annexin V, a marker of PS presentation in the outer membrane, was not stimulated by TNFα in *Rb1*-deficient uterine epithelial cells but in the control cells (Fig 6A and B), suggesting that TNFα-primed necroptosis in the uterine epithelium is controlled by *Rb1*. We investigated whether P_4, which promotes CCA in uterine epithelial cells during embryo implantation (Haraguchi *et al*, 2014), rescues TNFα-primed necroptosis in *Rb1*-deficient uterine epithelial cells. Supplementation of P_4 restored the responsiveness to TNFα and induced necroptosis in *Rb1*-deficient uterine epithelial cells (Fig 6A and B), suggesting that TNFα-primed epithelial necroptosis is controlled by CCA. Thymidine stimulates CCA in G1/S phase in many cell types (Harper, 2005; Chen & Deng, 2018), which was confirmed in primary mouse uterine epithelial cells (Fig EV4A). We next used thymidine to evaluate the role of CCA on TNFα-primed necroptosis in the uterine epithelial cells. We found that TNFα administration to *Rb1*-deleted cells does not increase the expression of annexin V, but the concomitant treatment of thymidine restores TNFα-primed expression of annexin V (Fig 6C and D), indicating that TNFα-primed epithelial necroptosis is regulated by CCA. Furthermore, we found that the expression of TNF receptor type 2 (TNFR2) is downregulated in *Rb1*-deleted epithelial cells, and the treatment of CCA inducers thymidine or P_4 upregulates its expression (Fig 6E). We confirmed that CCA promotes TNFα-primed necroptosis in a human endometrial epithelial cell line HEC151 (Fig EV4B–D), suggesting

Figure 3. *Rb1*$^{d/d}$ mice show persistent alignment of luminal epithelium surrounding the embryo, impaired trophoblast phagocytosis, and defected embryo invasion.

A Immunostaining of cytokeratin 8 (CK8), a marker of epithelial cell lineage, showed that epithelial alignment is collapsed and the trophoblast invades the stroma at implantation sites in *Rb1*$^{f/f}$ mice, while epithelial alignment is persistent and trophoblast invasion into the stroma is compromised in *Rb1*$^{d/d}$ mice. Scale bar = 200 μm; arrowhead, an embryo.

B Transmission electron microscopic analyses (TEM) showed that the uterine epithelium surrounding the embryo disappears and the trophoblast contacts directly with the stroma at 20:00 h on day 5 in *Rb1*$^{f/f}$ mice, while the uterine epithelium is persistent and the embryo does not attach to the stroma in *Rb1*$^{d/d}$ mice. Scale bar = 10 μm; red dotted line, stroma; green dotted line, luminal epithelium; blue dotted line, trophoblast.

C TEM showed that fragmented luminal epithelial cells with cytoplasmic lipid droplets are engulfed by the trophoblast in the control mice (*Rb1*$^{f/f}$ mice). Scale bar = 2 μm. Arrowhead, cytoplasmic fragments engulfed by trophoblast; yellow dotted line circle, cytoplasmic lipid droplets in the luminal epithelium; red dotted line, stroma; green dotted line, luminal epithelium; blue dotted line, trophoblast.

D TEM showed that the microvilli, markers of uterine receptivity, were observed at the surface of intact luminal epithelium on day 4 of pregnancy and epithelial cells with cytoplasmic lipid droplets were observed at 20:00 h on day 5 of pregnancy in the control mice (*Rb1*$^{f/f}$ mice). Scale bar = 2 μm; red dotted line, stroma; green dotted line, luminal epithelium; blue dotted line, trophoblast.

E Immunofluorescence of MFG-E8, a marker of programmed cell death, showed that MFG-E8 is not expressed at the implantation sites of *Rb1*$^{f/f}$ mice at 09:00 h on day 5 and *Rb1*$^{d/d}$ mice at 09:00 h and 20:00 h on day 5, but is expressed at the implantation sites of *Rb1*$^{f/f}$ mice at 20:00 h on day 5. Scale bar = 100 μm; blue signal, nuclei stained by DAPI; yellow signal, MFG-E8; arrowhead, embryo.

Data information: le, luminal epithelium; s, stroma; tr, trophoblast; n, nucleus.

© 2021 The Authors

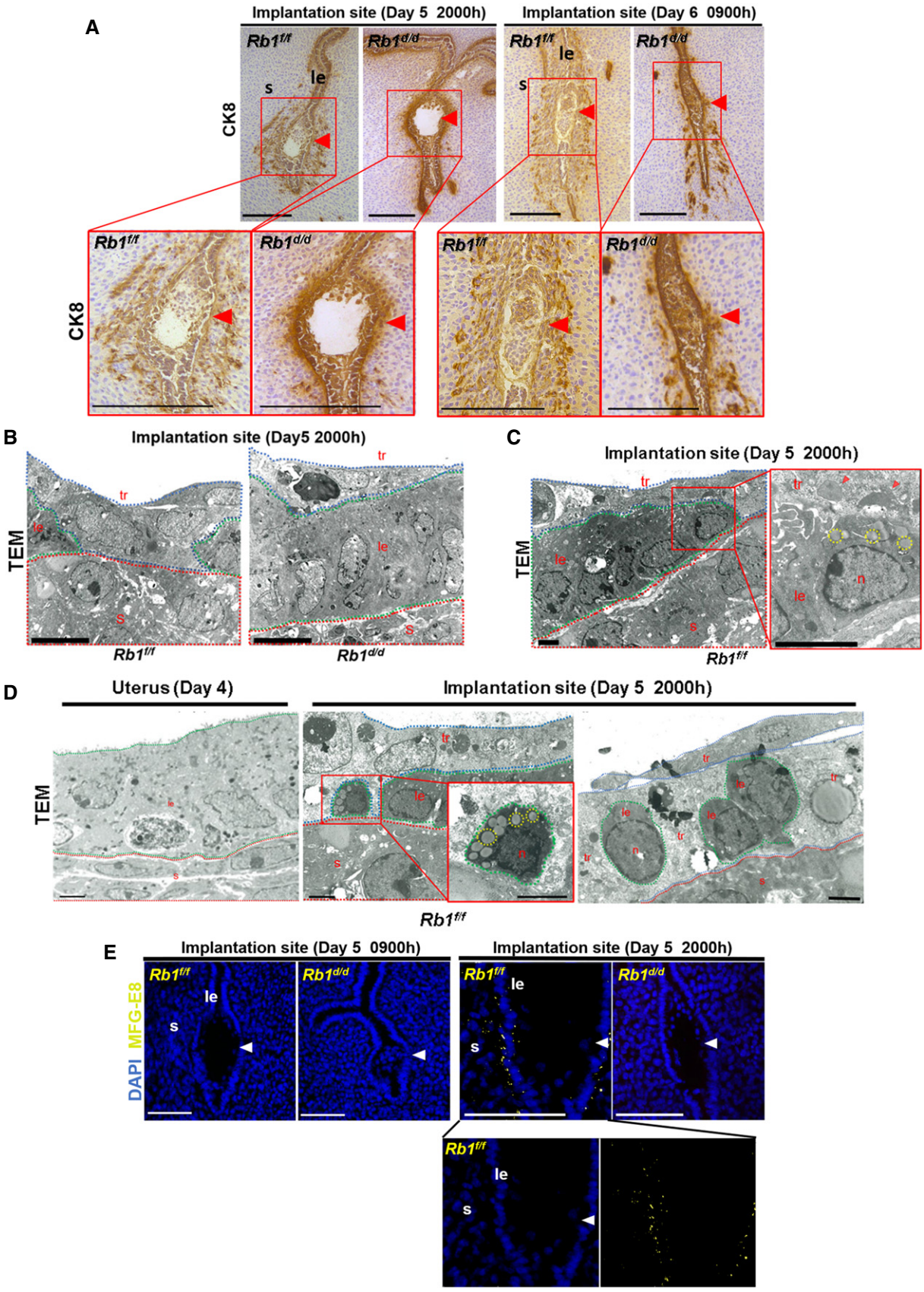
A
Implantation site (Day 5 2000h)
Implantation site (Day 6 0900h)
Rb1f/f
Rb1d/d
CK8
le
s
B
Implantation site (Day5 2000h)
TEM
tr
le
s
C
Implantation site (Day 5 2000h)
n
D
Uterus (Day 4)
Implantation site (Day 5 2000h)
E
Implantation site (Day 5 0900h)
Implantation site (Day 5 2000h)
DAPI MFG-E8

Figure 3.

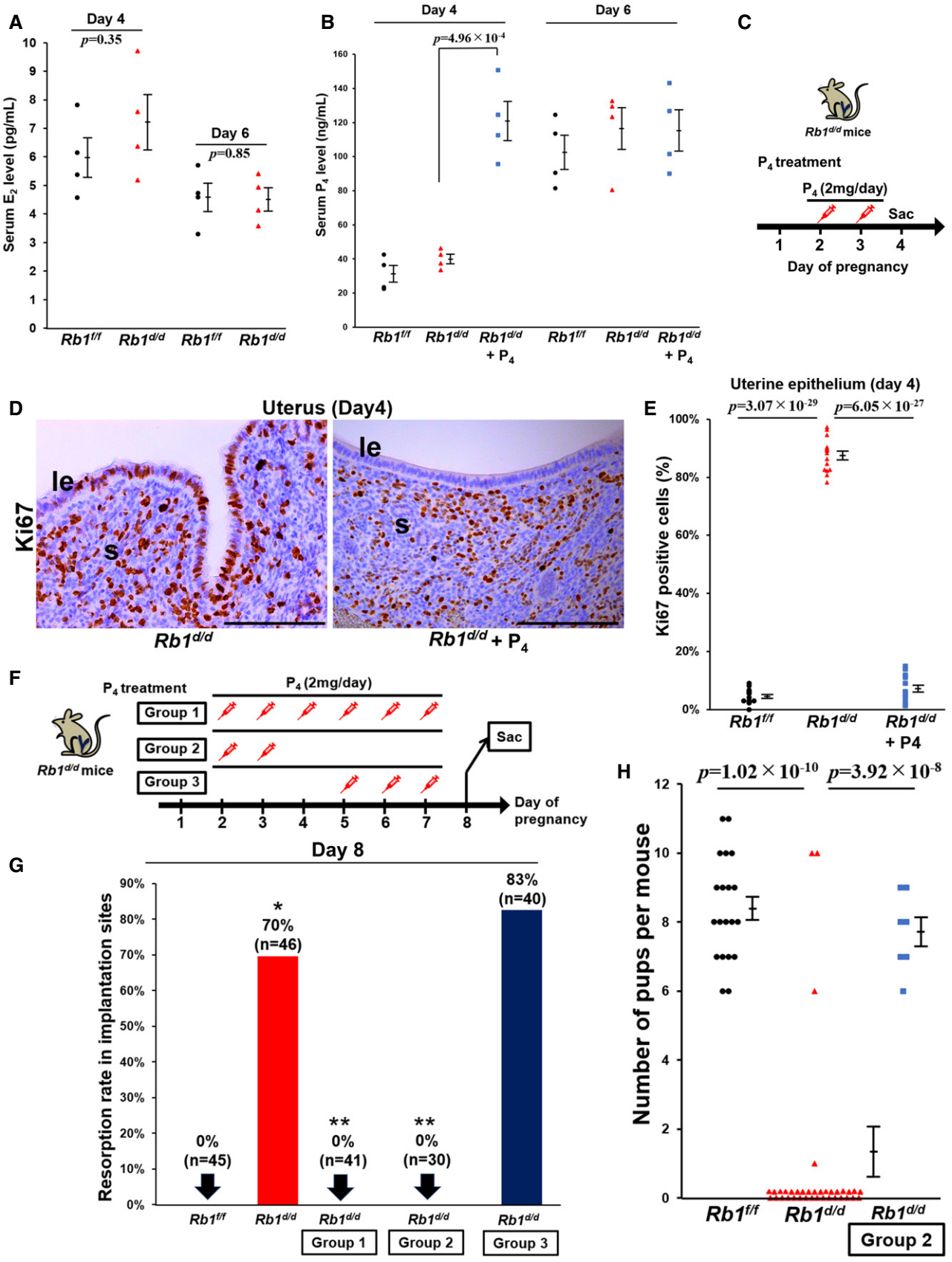

Figure 4.

© 2021 The Authors

Figure 4. Pre-implantation progesterone (P_4) supplementation is sufficient to normalize epithelial CCA and embryo invasion in *Rb1*$^{d/d}$ mice.

A Serum estradiol-17β (E_2) levels on days 4 and 6 of pregnancy were comparable between *Rb1*$^{f/f}$ and *Rb1*$^{d/d}$ mice (mean ± SEM, Student's *t*-test; $n = 4$ mice for each group).

B Serum P_4 levels on days 4 and 6 of pregnancy were comparable between *Rb1*$^{f/f}$ and *Rb1*$^{d/d}$ mice. In *Rb1*$^{d/d}$ mice, pre-implantation P_4 treatment on days 2 and 3 increased serum P_4 levels on day 4 but did not affect those on day 6 (mean ± SEM, Student's *t*-test; $n = 4$ mice for each group).

C Protocol of pre-implantation P_4 supplementation for the recovery of epithelial CCA in *Rb1*$^{d/d}$ mice. *Rb1*$^{d/d}$ mice underwent subcutaneous injection of P_4 (2 mg/day/mouse) on days 2 and 3, and sacrificed on day 4.

D Persistent Ki67 expression in the epithelium of *Rb1*$^{d/d}$ mice on day 4 was recovered by pre-implantation P_4 treatment on days 2 and 3. Scale bar = 100 μm; le, luminal epithelium; s, stroma.

E Ratio of Ki67-positive epithelial cells in *Rb1*$^{d/d}$ mice was completely suppressed by pre-implantation P_4 supplementation on days 2 and 3. The same data of *Rb1*$^{f/f}$ and *Rb1*$^{d/d}$ mice without P_4 treatment in Fig 2D were used (mean ± SEM, Student's *t*-test; $n = 5$ different mice for each group). Three different high-powered fields per mouse were analyzed, and each of the Ki67-positive ratios was demonstrated.

F Protocol of P_4 treatment for the recovery of embryo invasion and subfertility in *Rb1*$^{d/d}$ mice. P_4 (2 mg/day/mouse) was injected to *Rb1*$^{d/d}$ mice on days 2–7 in Group 1, on days 2 and 3 in Group 2, and on days 5–7 in Group 3.

G Resorption rate was reduced on day 8 in Groups 1 ($n = 41$ different implantation sites) and 2 ($n = 30$ different implantation sites), but not in Group 3 ($n = 40$ different implantation sites). The same data of *Rb1*$^{f/f}$ and *Rb1*$^{d/d}$ mice without P_4 treatment in Fig 2I were used. H&E staining was performed using all sections that show the implantation sites, and resorption rate was evaluated. *$P < 0.05$ vs. *Rb1*$^{f/f}$ mice; **$P < 0.05$ vs. *Rb1*$^{d/d}$ mice; Fisher's exact test.

H Number of pups delivered by *Rb1*$^{d/d}$ dams was normalized by pre-implantation P_4 treatment on days 2 and 3 (Group 2) (mean ± SEM, Student's *t*-test). The same data of *Rb1*$^{f/f}$ and *Rb1*$^{d/d}$ dams without P_4 treatment in Fig 1E were used. The numbers of pups in 20 *Rb1*$^{f/f}$ and 37 *Rb1*$^{d/d}$ dams without P_4 treatment and 7 *Rb1*$^{d/d}$ dams with P_4 treatment were evaluated.

CCA-induced necroptosis is a common phenomenon in the cells whose growth is ovarian hormone-dependent. These findings indicate that *Rb1*-induced CCA of uterine epithelial cells contributes to TNFα-primed necroptosis by the upregulation of TNFR2. We believe that this is a novel physiological machinery of luminal epithelium elimination during embryo invasion.

Pre-implantation P_4 rescues necroptosis of the luminal epithelium at the implantation site in Rb1$^{d/d}$ mice

We examined whether P_4 supplementation recovers epithelial necroptosis in *Rb1*$^{d/d}$ mice. Pre-implantation administration of P_4 recovered the fragmented cytoplasm with lipid droplets in the luminal epithelium and trophoblast engulfment (Fig 7A) and normalized the expression of MFG-E8 and pRIP3 in the luminal epithelium of *Rb1*$^{d/d}$ mice (Fig 7B and C). These findings suggest that P_4 rescues epithelial CCA and necroptosis, trophoblast engulfment, and subsequent embryo invasion in *Rb1*$^{d/d}$ mice.

Rb1 deletion in the luminal epithelium skews cell cycle-related genes

To examine the influence of *Rb1* and P_4 on transcriptome in the luminal epithelium, we performed RNA-seq using day 4 luminal epithelium dissected out from *Rb1*$^{f/f}$ mice and *Rb1*$^{d/d}$ mice with and without P_4 supplementation by laser capture microdissection (LCM). We found 2,185 differentially expressed genes (DEGs) which showed $\log_2$-fold changes ≥ 1 in at least one group compared with others (Fig EV5A). Among 10 unique clusters defined by K-means clustering, we focused on the gene cluster 6 in which the transcripts are poorly expressed especially in *Rb1*$^{d/d}$ mice without P_4 supplementation compared with other groups. To examine the feature of the cluster 6, we examined the profile of the genes which belong to this cluster using publicly available database of RNA-seq and ChIP-seq regarding transcriptional factors (TFs). We found that DEGs in this cluster are poorly correlated with PGR but highly correlated with cell cycle-related TFs such as serum response factor (SRF) and E2F8 (Fig EV5B). In addition, gene ontology (GO) analyses also revealed that the cluster 6 is related to epithelial differentiation and inhibition of cell proliferation (Fig EV5C). These results indicate that P_4 administration to *Rb1*$^{d/d}$ mice rescues embryo invasion failure by specifically influencing the cell proliferation pathway of the luminal epithelium. Among cell cycle-associated genes, mRNAs of cyclin-dependent kinase inhibitors *Cdkn1a* and *Cdkn2c* were downregulated by *Rb1* deletion and upregulated by P_4 treatment, suggesting that CCA in the luminal epithelium is regulated by *Cdkn1a* and *Cdkn2c* (Fig EV5D). Consistent with RNA-seq results, CDKN2c protein was expressed less in *Rb1*$^{d/d}$ mice compared with *Rb1*$^{f/f}$ mice, and exogenous P_4 increased CDKN2c expression in *Rb1*$^{d/d}$ mice (Fig EV5E). Cyclin-dependent kinase inhibitors Cdkn1a and Cdkn2c might work together in epithelial necroptosis.

Stromal Rb1 controls epithelial proliferation and embryo invasion in cooperation with epithelial Rb1

We found that RB is localized in the epithelium and stroma on day 4. These findings indicate the roles of *Rb1* not only in the epithelium but in the stroma during the peri-implantation period. To clarify the

Figure 5. Necroptosis of luminal epithelium at the implantation sites is observed in *Rb1*$^{d/d}$ mice.

A pRIP3, a central mediator of necroptosis, was not expressed at the implantation sites of *Rb1*$^{d/d}$ mice but was expressed at those of *Rb1*$^{f/f}$ mice at 15:00 h on day 5. Scale bar = 100 μm; blue signal, nuclei stained by DAPI; purple signal, pRIP3; le, luminal epithelium; s, stroma; arrowhead, embryo; green dotted line, luminal epithelium; red dotted line, stroma.

B TNFα stimulated the expression of pMLKL, a critical mediator of necroptosis, in the primary mouse uterine epithelial cells. Scale bar = 50 μm; blue signal, nuclei stained by DAPI; red signal, pMLKL.

C Uterine expression of *TNFα* was elevated in the control mice (*Rb1*$^{f/f}$ mice) on days 5 and 6 compared with on day 4 (mean ± SEM, Student's *t*-test; $n = 3$ mice for each group). As for the uterine samples on days 5 and 6, those with implantation sites were examined.

D The implanting embryo and the uterus produced TNFα at the implantation site of both *Rb1*$^{f/f}$ and *Rb1*$^{d/d}$ mice. Immunostaining of TNFα at the implantation sites of *Rb1*$^{f/f}$ and *Rb1*$^{d/d}$ mice were performed. Scale bar = 100 μm; arrowhead, embryo.

© 2021 The Authors

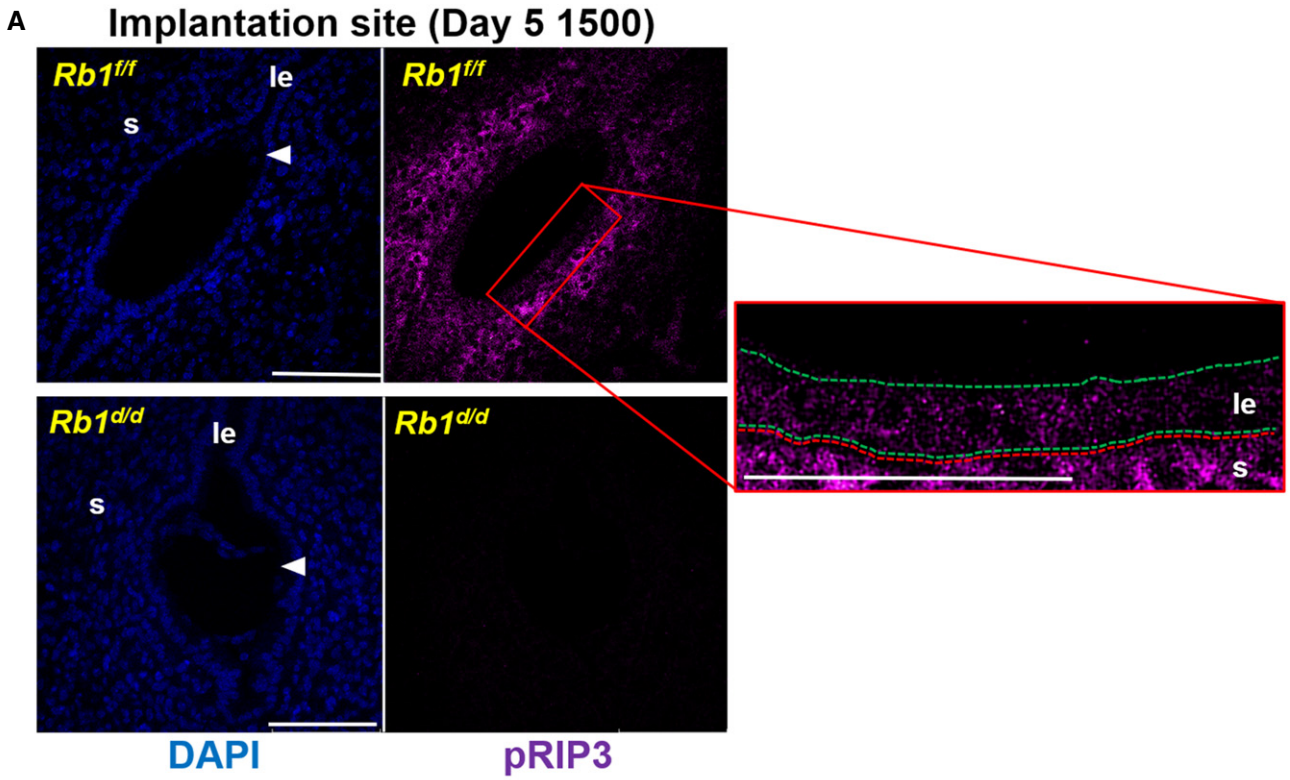

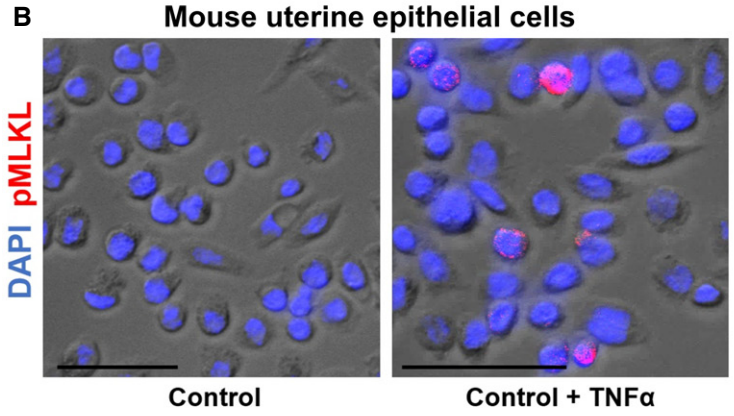

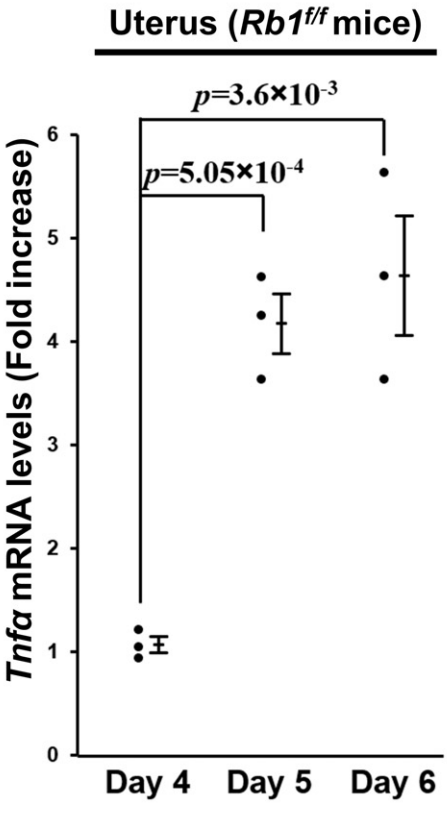

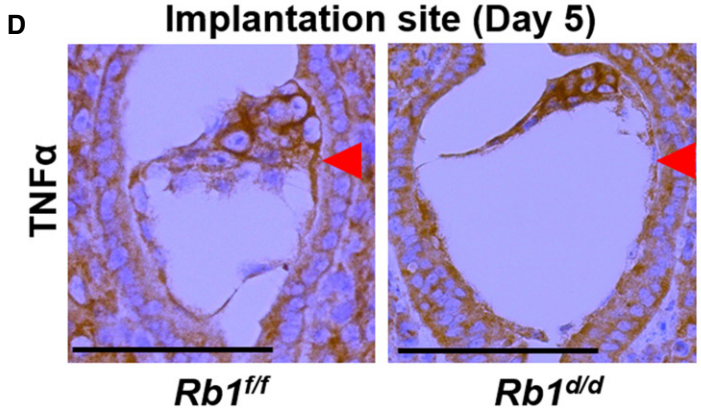

Figure 5.

© 2021 The Authors

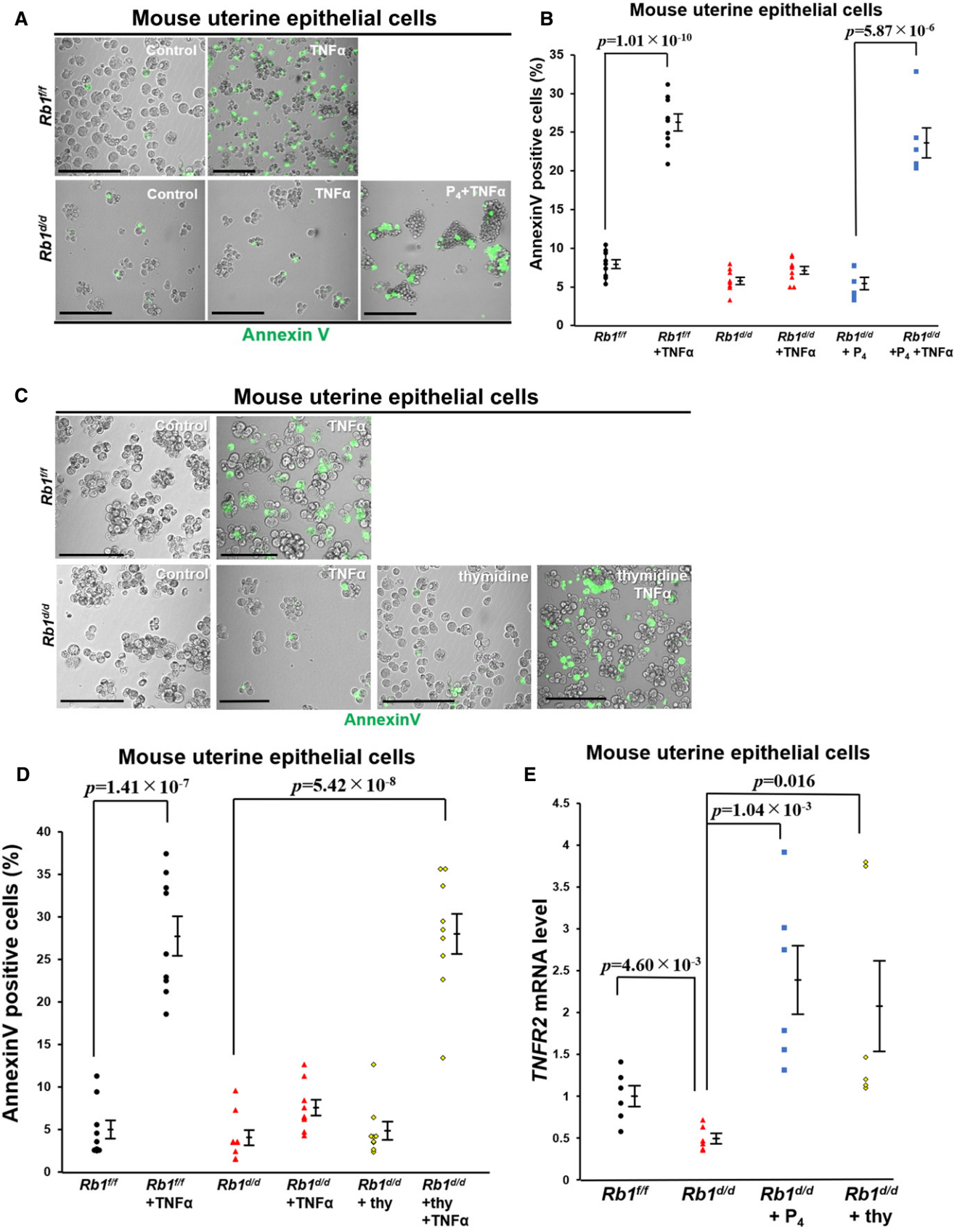
A
Mouse uterine epithelial cells
Control
TNFα
Rb1f/f
Rb1d/d
P4+TNFα
Annexin V
B
Mouse uterine epithelial cells
p=1.01 × 10-10
p=5.87 × 10-6
AnnexinV positive cells (%)
Rb1f/f
Rb1f/f +TNFα
Rb1d/d
Rb1d/d +TNFα
Rb1d/d + P4
Rb1d/d +P4 +TNFα
C
Mouse uterine epithelial cells
thymidine
thymidine TNFα
AnnexinV
D
Mouse uterine epithelial cells
p=1.41 × 10-7
p=5.42 × 10-8
AnnexinV positive cells (%)
Rb1d/d + thy
Rb1d/d +thy +TNFα
E
Mouse uterine epithelial cells
p=0.016
p=1.04 × 10-3
p=4.60 × 10-3
TNFR2 mRNA level

Figure 6.

Figure 6. CCA of uterine epithelial cells contributes to susceptibility to TNFα and TNFα-primed necroptosis through TNF receptor type 2.

A, B *In vitro* analyses using primary mouse uterine epithelial cells demonstrated that TNFα induces the expression of annexin V, a marker of PS presentation at the outer membrane of $Rb1^{f/f}$ epithelial cells but does not in $Rb1^{d/d}$ ones, and P_4 restores TNFα-primed annexin V expression in $Rb1^{d/d}$ uterine epithelial cells (mean ± SEM, Student's *t*-test). Using three lines of primary mouse epithelial cells obtained from both $Rb1^{f/f}$ and $Rb1^{d/d}$ mice, the *in vivo* experiments were performed three times. Each of the annexin V-positive ratios was demonstrated. Scale bar = 100 μm; green signal, annexin V.

C, D Annexin V assay using primary mouse uterine epithelial cells showed that TNFα administration increases the expression of annexin V in growth-arrested mouse epithelial cells with thymidine treatment, but does not in the control cells (mean ± SEM, Student's *t*-test). Using three lines of primary mouse epithelial cells obtained from both $Rb1^{f/f}$ and $Rb1^{d/d}$ mice, the *in vivo* experiments were performed three times. Each of the annexin V-positive ratios was demonstrated. Scale bar = 100 μm; green signal, annexin V.

E The expression of TNF receptor type 2 (TNFR2) was upregulated in growth-arrested epithelial cells with thymidine and P_4 supplementation (mean ± SEM, Student's *t*-test). Using three lines of primary mouse epithelial cells obtained from both $Rb1^{f/f}$ and $Rb1^{d/d}$ groups, qPCR was performed in duplicate.

role of epithelial *Rb1* in embryo implantation, we generated epithelial *Rb1*-deleted mice (*Rb1* eKO) by crossing *Rb1*-loxP mice with *Ltf*-Cre mice. Cre-negative homozygous littermate female mice for the conditional alleles were used as controls (*Rb1* eControl). Although RB was efficiently deleted in the uterine epithelium of *Rb1* eKO mice (Fig 8A), *Rb1* eKO female mice showed normal fertility (Fig 8B). Notably, epithelial CCA on day 4 was normal in *Rb1* eKO mice (Fig 8C), suggesting that stromal *Rb1* controls epithelial cell proliferation and embryo invasion in cooperation with epithelial *Rb1* during embryo implantation.

Appropriate CCA of the luminal epithelium is associated with embryo implantation outcome in patients undergoing infertility treatment

We investigated cell cycle status at the time of implantation in human endometria obtained from patients undergoing IVF-ET treatment to evaluate the correlation between the extent of epithelial CCA and the clinical outcome of embryo transfer following endometrial biopsy. The ratio of Ki67-positive staining was low in the group of patients with successful clinical pregnancy compared with that of patients without pregnancy (Fig 9A and B), suggesting that CCA in the uterine luminal epithelium is involved in human embryo implantation.

Discussion

In the present study, we found that uterine deficiency of *Rb1* results in persistent cell cycle progression of the luminal epithelium until embryo attachment, failure in the disappearance of luminal epithelial cells during embryo invasion, defects in the presentation of PS on the outer membrane of luminal epithelial cells, and loss of luminal epithelium necroptosis with trophoblast phagocytosis, suggesting that CCA of the uterine luminal epithelium stimulates necroptosis during embryo invasion. Importantly, we also found that thymidine- and P_4-induced CCA recovers TNFα-primed necroptosis through the induction of TNFR2 in *Rb1*-deficient epithelial cells. Pre-implantation P_4 administration normalizes the cell cycle status of the luminal epithelium at the time of embryo attachment, induces epithelial necroptosis with trophoblast phagocytosis during embryo invasion, and finally rescues embryo invasion in uterine *Rb1* null mice. These findings indicate that proper CCA and necroptosis in uterine luminal epithelium are precisely regulated by *Rb1* and P_4 during implantation, which results in successful embryo invasion (Fig 9C). In addition, epithelial CCA at the time of attachment is associated with successful implantation in humans.

Necroptosis, a relatively new concept of non-apoptotic programmed cell death, is augmented by TNFα which activates the RIP1-RIP3-MLKL axis by phosphorylation (Guo *et al*, 2009), and phosphorylated MLKL (pMLKL) drills the cellular membrane like necrosis (Zhu *et al*, 2016). The initial disappearance of the luminal epithelium barrier surrounding the blastocyst occurs at the lateral sides of the implantation chamber. Our previous study has revealed that apoptosis of the luminal epithelium is not a key mechanism for the initial step of the luminal epithelium disappearance around the embryo (Matsumoto *et al*, 2018). A recent study demonstrated that entosis, a non-apoptotic form of cell death with cell-in-cell formation (Overholtzer *et al*, 2007), is involved in this process in which a live trophoblast cell engulfs and kills an entire live luminal epithelial cell to remove the luminal epithelium barrier (Li *et al*, 2015). The present study revealed that at the lateral sides of the implantation chamber, PS is exposed at the outer membranes of luminal epithelium, pRIP3 is expressed in the cytoplasm of luminal epithelium, and dying epithelial cells are engulfed by the neighboring trophoblast cells. It has been reported that PS exposure is observed in not only apoptotic but non-apoptotic cell death including necroptosis and entosis, and pRIP3 is a specific marker of necroptosis, and phagocytes engulf live cells in the process of entosis and dying cells in the processes of apoptosis and necroptosis (Segawa *et al*, 2018; Shlomovitz *et al*, 2019; Tang *et al*, 2019). Our findings indicate that necroptosis is involved in luminal epithelium elimination at the lateral sides of the implantation chamber during the initial disappearance of luminal epithelium, which is a similar physiological

Figure 7. Pre-implantation P_4 administration recovers epithelial necroptosis and trophoblast phagocytosis at the implantation site in $Rb1^{d/d}$ mice.

A In $Rb1^{d/d}$ mice with pre-implantation P_4 treatment, the fragmented uterine epithelial cells with the cytoplasmic lipid droplets were engulfed by the trophoblast cells. Scale bar = 2 μm. Arrowhead, cytoplasmic fragments engulfed by trophoblast; dotted line circle, lipid droplets in the cytoplasm; tr, trophoblast; le, luminal epithelium; s, stroma; red dotted line, stroma; green dotted line, luminal epithelium; blue dotted line, trophoblast.

B Pre-implantation P_4 treatment rescued the expression of MFG-E8 on day 5 of pregnancy in $Rb1^{d/d}$ uteri. Scale bar = 100 μm. Blue signal, nuclei stained by DAPI; yellow signal, MFG-E8; le, luminal epithelium; s, stroma; arrowhead, embryo.

C Pre-implantation P_4 treatment recovered the expression of pRIP3, a mediator of necroptosis, on day 5 of pregnancy in $Rb1^{d/d}$ uteri. Scale bar = 100 μm; blue signal, nuclei stained by DAPI; purple signal, pRIP3; le, luminal epithelium; s, stroma; arrowhead, embryo.

© 2021 The Authors

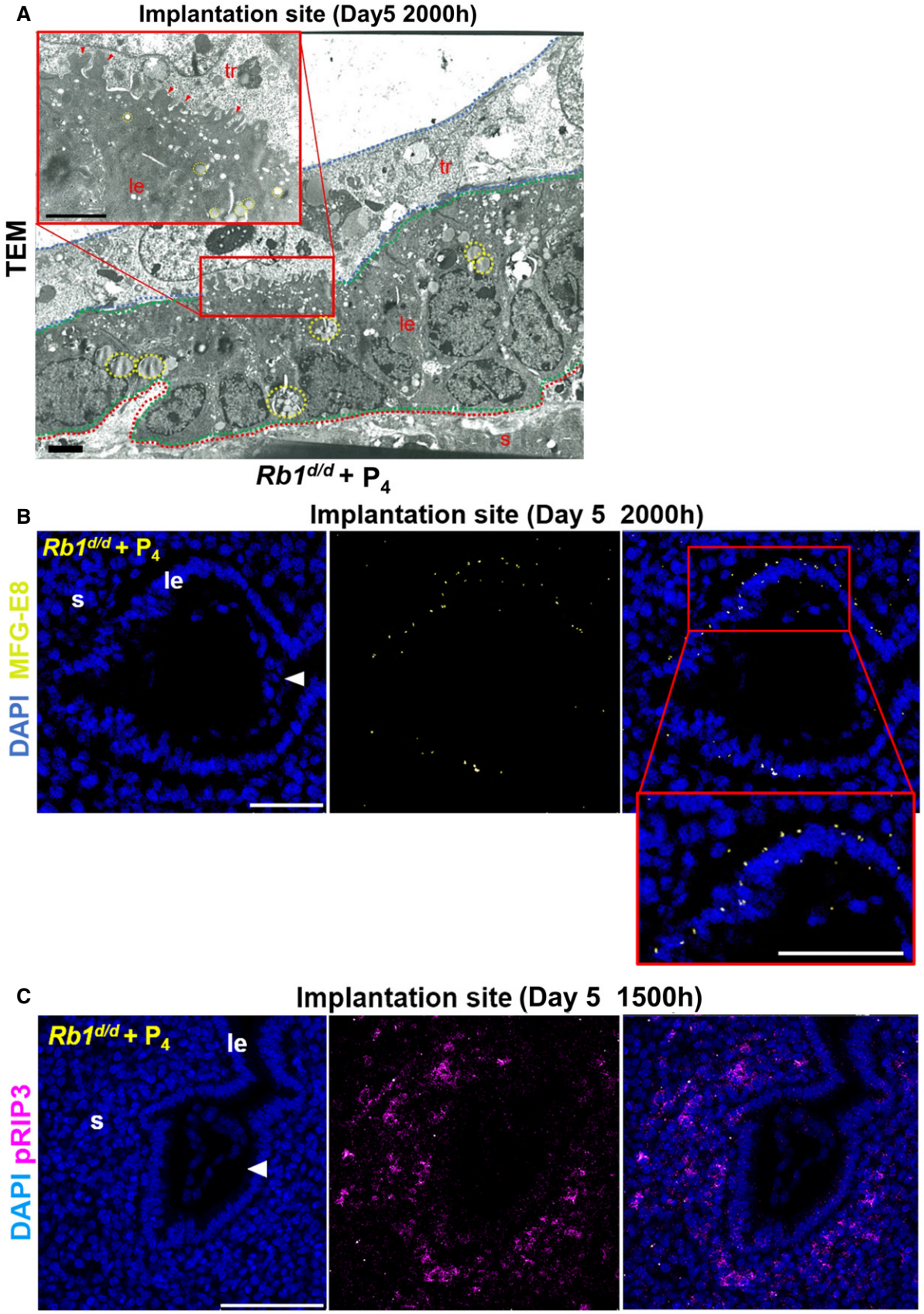
A
Implantation site (Day5 2000h)
TEM
tr
le
tr
le
s
Rb1d/d + P4
B
Implantation site (Day 5 2000h)
Rb1d/d + P4
le
s
DAPI MFG-E8
C
Implantation site (Day 5 1500h)
Rb1d/d + P4
le
s
DAPI pRIP3

Figure 7.

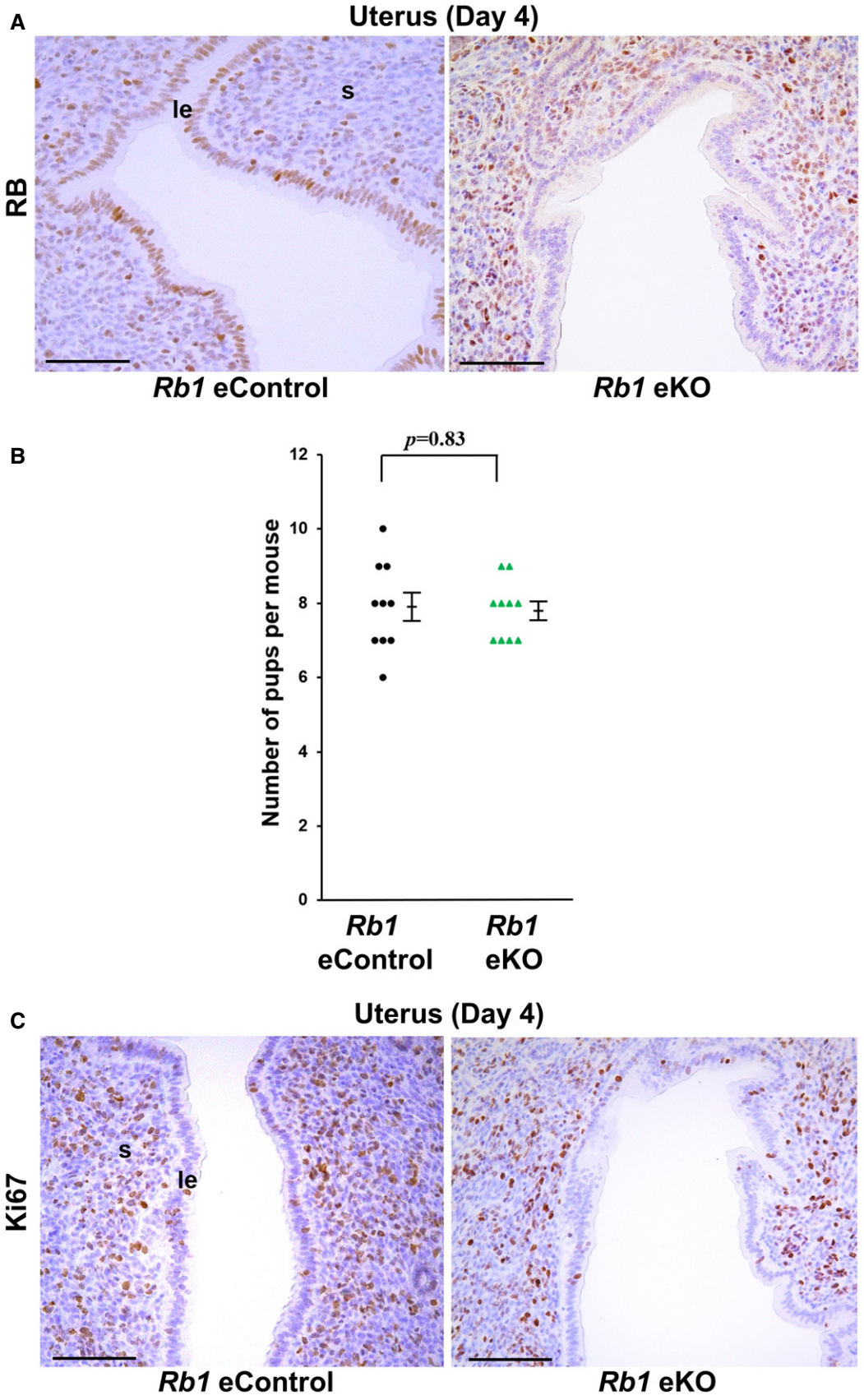

Figure 8.

© 2021 The Authors

Figure 8. Stromal *Rb1* controls epithelial proliferation and embryo invasion in cooperation with epithelial *Rb1*.

A RB was efficiently deleted in the uterine epithelium of uterine epithelium-specific conditional knockout mice (*Rb1* eKO mice). Scale bar = 100 μm. *Rb1* eKO mice, $Rb1^{loxP/loxP}Ltf^{Cre/+}$ mice; *Rb1* eControl mice (littermate controls of *Rb1* eKO mice), $Rb1^{loxP/loxP}$ mice; le, luminal epithelium; s, stroma.

B Number of new-born pups was comparable between *Rb1* eKO and eControl dams (mean ± SEM, Student's *t*-test; $n = 10$ different dams for each group).

C The expression patterns of Ki67 on day 4 in uterine epithelium were comparable between *Rb1* eKO and *Rb1* eControl mice. Scale bar = 100 μm; le, luminal epithelium; s, stroma.

phenomenon to synaptic pruning (Chechik *et al*, 1999). Given that epithelial entosis occurs at the lateral sides of the implantation chamber where epithelial necroptosis takes place, at least it is certain that non-apoptotic cell death mechanisms including necroptosis and entosis play major roles in the initial step of luminal epithelium barrier removal during embryo invasion. In the following step, apoptosis occurs in the luminal epithelium at the anti-mesometrial side (Joswig *et al*, 2003; Li *et al*, 2015). Apoptotic and non-apoptotic cell death mechanisms regulate the luminal epithelium disappearance in the spaciotemporal manners.

Uterine stromal–epithelial communication contributes to successful embryo implantation. The basic helix–loop–helix transcription factor *Hand2* in the uterine stroma suppresses the production of fibroblast growth factors that act as paracrine inducers of estrogen-dependent epithelial proliferation in the peri-implantation period (Li *et al*, 2011), suggesting that stromal *Hand2* is in charge of P_4-dependent communication from stroma to epithelium. Previous studies reported by us and others suggested that uterine stroma regulates embryo invasion through detachment of the luminal epithelium (Schlafke & Enders, 1975; Matsumoto *et al*, 2018). Our recent study demonstrated that stromal HIF2α, a major transcriptional factor inducible by low oxygen tension, contributes to trophoblast invasion by inducing the expression of MT2-MMP, lysyl oxidase, VEGF, and adrenomedullin, provoking the luminal epithelium detachment from the stroma, and activating the embryonic PI3K-AKT pathway (Matsumoto *et al*, 2018). The present study showed that stromal *Rb1* works in cooperation with epithelial *Rb1* to regulate epithelial CCA and embryo invasion. These findings reinforce the critical stromal functions for embryo invasion. GO analysis demonstrated that the gene cluster in which the transcripts were downregulated in the luminal epithelium of $Rb1^{d/d}$ mice without P_4 treatment compared with other groups was not related to inflammation but to epithelial differentiation and inhibition of cell proliferation (Fig EV5C), suggesting the pathological processes other than inflammation in the luminal epithelium may cause embryo invasion failure in $Rb1^{d/d}$ mice.

Dying cells exude PS at their outer membranes to enable detection by phagocytic cells, which is called an "eat-me signal" (Hanayama *et al*, 2002). MFG-E8 secreted by phagocytic cells binds PS at the outer membrane and is therefore used for a marker of eat-me signals (Hanayama *et al*, 2002). In addition, eat-me signals are activated in not only apoptosis but necroptosis which TNFα promotes (Guo *et al*, 2009; Ehrhardt *et al*, 2013; Zargarian *et al*, 2017). This study revealed that the implanting embryo and uterus at the implantation site produce TNFα which promotes the presentation of PS at the outer membrane in the luminal epithelium, and MFG-E8 is present at the outer membrane of the luminal epithelium. This indicates that TNFα produced at the implantation site stimulates necroptosis of the luminal epithelial cells, and MFG-E8 facilitates the trophoblast seeking out dying luminal epithelial cells and finally engulfing the cytoplasmic fragments of luminal epithelial cells at the embryo–uterine interface. Therefore, we believe that TNFα and MFG-E8 are involved in epithelial necroptosis, and these molecular and cellular interactions between the luminal epithelium and trophoblast are critical for embryo invasion.

Ki67 is not expressed in the nucleus during the G0 stage when the cell cycle is arrested (Schwarting *et al*, 1986). We found that Ki67-positive cells of the luminal epithelium decrease in the process of normal implantation on day 4, and the proliferating epithelial cells remain persistent in *Rb1* null mice with failed epithelial necroptosis and embryo invasion. Cells with CCA are susceptible to TNFα, which promotes cell death (Ehrhardt *et al*, 2013; Zargarian *et al*, 2017). The current study revealed that TNFα is abundantly produced at the implantation site and CCA inducers thymidine and P_4 rescue TNFα-primed necroptosis in *Rb1*-deficient growth-arrested uterine epithelial cells through the upregulation of TNFR2. These findings indicate that the luminal epithelium with *Rb1*- and P_4-induced CCA is susceptible to implantation site-derived TNFα, which induces epithelial necroptosis and embryo invasion.

Influence of P_4 during pregnancy remains elusive, and it is unclear how P_4 supports successful embryo implantation. P_4 inhibits estrogen-induced cell cycle progression of endometrial epithelial cells, which is a fundamental role of P_4 to prevent endometrial cancer as well as an infertility treatment for the luteal phase of hormonal support. Our study revealed novel mechanisms in which RB and P_4 regulate endometrial epithelial CCA and necroptosis precisely and lead to successful embryo invasion. This study may improve understanding of both molecular and cellular aspects of embryo implantation in humans.

Figure 9. CCA of uterine luminal epithelial cells is a hallmark of embryo implantation in mice and humans.

A Representative pictures of Ki67 staining in the human endometria obtained from women at the time of embryo implantation. Samples were divided into two groups according to the outcome of clinical pregnancy following endometrial biopsy. Scale bar = 100 μm; le, luminal epithelium; s, stroma.

B Ratio of Ki67-positive cells in the human uterine luminal epithelium during the implantation period was lower in the group with pregnancy than the group without pregnancy (mean ± SEM, Student's *t*-test; $n = 10$ different individuals for each group). Three different high-powered fields per sample were analyzed and each of the Ki67-positive ratios was demonstrated.

C Potential processes that contribute to embryo invasion through uterine RB-induced CCA and necroptosis of luminal epithelial cells.

© 2021 The Authors

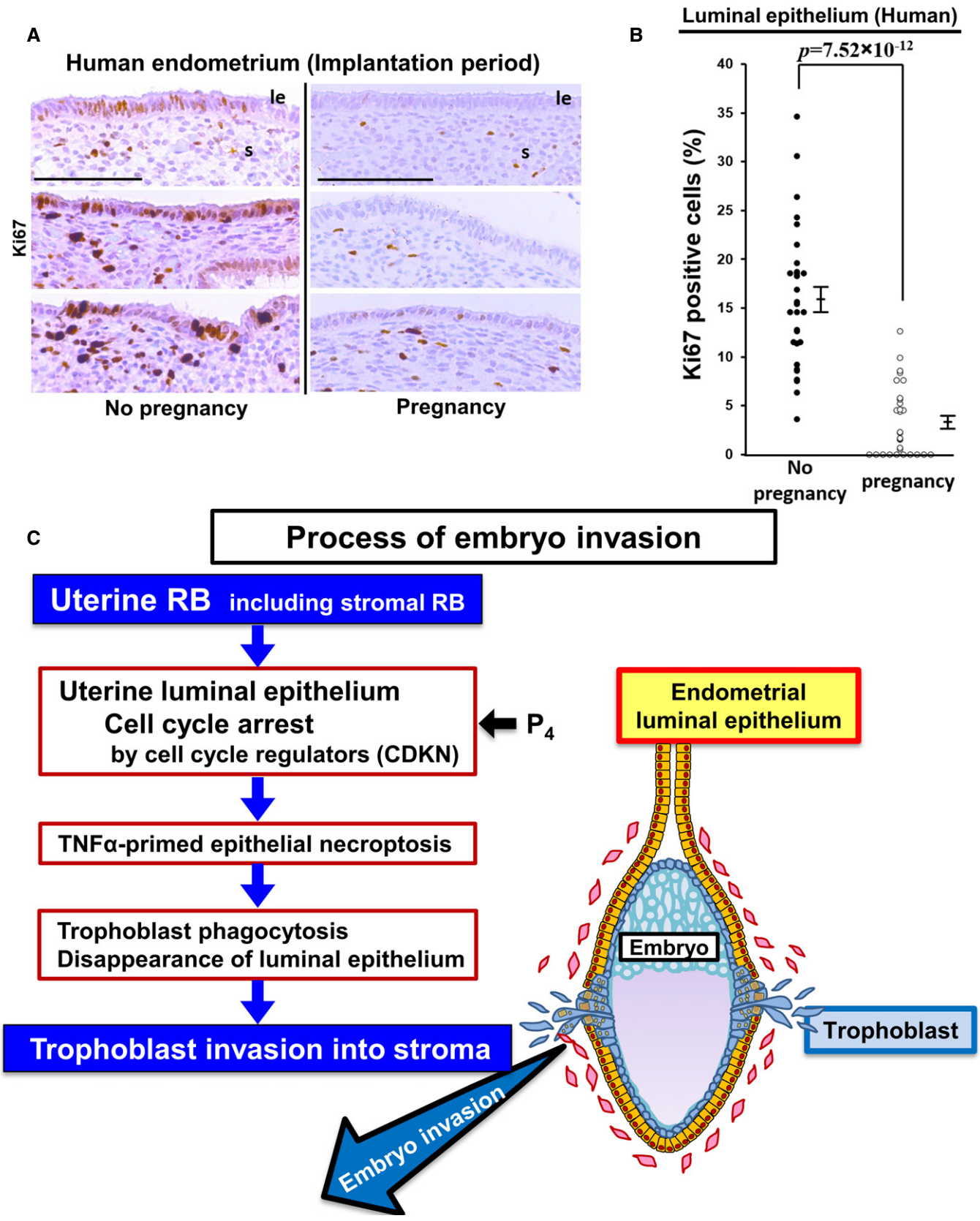

Figure 9.

© 2021 The Authors

Materials and Methods

Mice

WT mice (C57BL/6J, SLC, Hamamatsu, Japan), *Pgr*-Cre mice (Soyal *et al*, 2005), *Ltf*-Cre mice (Daikoku *et al*, 2014), and *Rb1*-floxed mice (Marino *et al*, 2000) were used in this study. *Ltf* and *Pgr* are expressed in the luminal epithelium and all the layers of uterus, respectively. In *Ltf*-Cre female mice, Cre recombinase is specifically expressed in the uterine epithelium (Daikoku *et al*, 2014). In the previous study, the floxed gene was specifically deleted in the uterine epithelium of the pregnant mouse model using *Ltf*-Cre female mice (Matsumoto *et al*, 2018). In *Pgr*-Cre female mice, Cre recombinase is expressed not only in the uterus but in the ovary (Soyal *et al*, 2005). Although *Pgr*-Cre mouse line can be used for deletion of the floxed gene in the entire uterus (Matsumoto *et al*, 2018), the events regulated by ovarian functions such as ovulation and fertilization need to be evaluated in the pregnant mouse models using *Pgr*-Cre females (Haraguchi *et al*, 2019). Mice with deletion of *Rb1* in the whole uterus ($Rb1^{d/d}$ mice) were generated by crossing *Pgr*-Cre with *Rb1*-floxed mice. Mice with deletion of *Rb1* in the uterine epithelium (*Rb1* eKO mice) were generated by crossing *Rb1*-floxed mice with *Ltf*-Cre mice. Cre-negative homozygous littermates for the conditional alleles were used as controls. All mice used in this investigation were housed in the University of Tokyo Animal Care Facility according to the institutional guidelines for the use of laboratory animals. The experimental procedures were approved by the institutional animal experiment committee.

Analysis of pregnancy events

For the evaluation of pregnancy phenotypes, female mice of each line (2-to 5-month-old) were mated with fertile males, and day 1 of pregnancy was defined as the day when we recognized a vaginal plug. Ovulation, fertilization, pre-implantation embryo development, and implantation were assessed as described (Hirota *et al*, 2010; Matsumoto *et al*, 2018). Daily subcutaneous injections of P_4 (2 mg/mouse/day) to $Rb1^{d/d}$ mice were performed from day 2 of pregnancy or from day 5 of pregnancy. Daily P_4 injection at the dose of 2 mg/day/mouse was used for the induction of embryo implantation in delayed implantation mouse model (Yoshinaga & Adams, 1966; Huet & Dey, 1987; Ma *et al*, 2003). In our previous study, we confirmed that daily administration of P_4 at the dose of 2 mg/day/mouse from day 2 is not harmful for embryo implantation in WT mice (Matsuo *et al*, 2020).

Human tissues

Endometrial tissues were obtained from infertile patients planning to undergo IVF-ET treatment. As the limitation of the experiments using human subjects, it is practically impossible to perform human endometrial biopsy in the implantation period of the embryo transfer cycle. Since the endometrial genes related to uterine receptivity are expressed in a reproducible fashion among the cycles (Diaz-Gimeno *et al*, 2013), we consider that the uterine receptivity-associated uterine cell proliferation status in the cycle prior to the embryo transfer cycle corresponds to that in embryo transfer cycle. Thus, we substituted the endometria in the cycle prior to embryo transfer instead. Endometrial biopsy was performed at the 7^{th} day of P_4 treatment in an artificial cycle which is considered as the implantation period in humans. To minimize the differences of hormonal conditions among the individual patients, the same protocol of artificial hormonal treatment in the cycle of endometrial biopsy was used for all the patients. The patients underwent embryo transfer in the following artificial cycles after endometrial biopsy. We investigated the relationship between the peri-implantation uterine cell proliferation status and the pregnancy outcome. The samples were divided into two groups according to the outcome of clinical pregnancy following endometrial biopsy. Endometrial samples were evaluated by immunostaining of Ki67. Experimental procedures were approved by the institutional review board of the University of Tokyo (IRB number: 10991), and signed informed consent for the use of tissues was obtained from each patient. The experiments were performed according to the principles in the WMA Declaration of Helsinki and the Department of Health and Human Services Belmont Report.

H&E staining, immunostaining, and fluorescence assay

H&E staining, immunohistochemistry, and fluorescence assay using frozen sections (12 μm), or formalin-fixed paraffin-embedded sections (6 μm), were performed as described previously (Matsumoto *et al*, 2018). Antibodies to Ki67 (SP6, Thermo Fisher Scientific, Cheshire, UK 1:400), and pSTAT3 (EP2147Y, Abcam, Cambridge, UK 1:300), COX2 (AA570-598, Cayman, Ann Arbor, MI, USA 1:200), CK8 (AB531826, DSHB, Iowa City, IA, USA 1:100), RB (ab181616, Abcam, 1:200), pRB (8516, Cell Signaling Technology, Beverly, MA, USA, 1:200), TNFα (BS1857, Bioworld Technology, Nanjing, China 1:500), ERα (ab80922, Abcam, 1:400), PGR (ab63605, Abcam, 1:200), and FOXO1 (2880S, Cell Signaling Technology, 1:200) were used.

Measurement of serum P_4 and E_2 levels

Blood samples from mice were collected on the indicated days of pregnancy. Serum P_4 and E_2 levels were measured as described previously (Matsumoto *et al*, 2018). Serum P_4 levels were measured by Progesterone EIA kit (582601, Cayman), and E_2 levels were measured by Estradiol ELISA kit (ES180S-100, CalBiotech, Spring Valley, CA, USA).

Transmission Electron Microscopy (TEM)

TEM was performed as described previously (Matsumoto *et al*, 2018).

Culture of primary mouse uterine epithelial cells

Mouse uterine epithelial cells are obtained from $Rb1^{f/f}$ and $Rb1^{d/d}$ mice on day 4 of pregnancy. Briefly, uterine tissues were incubated with pancreatin (Sigma-Aldrich, St. Louis, MO, USA) and dispase (Fuji Film Wako Pure Chemicals, Osaka, Japan) in HBSS at 4°C for 30 min, at room temperature for 30 min and then, at 37°C for 4 min. The tissue debris was removed by centrifugation, and the supernatant was passed through 70 μm cell strainer, and the epithelial cells were collected on the mesh of the cell strainer. The cells were seeded in collagen I-coated plate and cultured in MEM with 10%

© 2021 The Authors

charcoal-stripped FBS for 2 days. Cultured epithelial cells were pre-incubated in the media with or without 10^{-7} M of P_4 for 1 h and then incubated in those with or without 60 ng/ml of mouse recombinant TNFα (Sigma-Aldrich) for 4 h at 37°C. To induce CCA in the primary mouse uterine epithelial cells, the method of double thymidine block was used (Chen & Deng, 2018). Briefly, the cells were seeded in plastic plate and cultured in MEM with 5% charcoal-stripped FBS. As the first round of thymidine block, the cultured cells were incubated in the media with or without 2 mM thymidine (Sigma-Aldrich) for 18 h and incubated in the fresh media for 9 h. As the second round of thymidine block, the cells were incubated again in the media with or without 2 mM thymidine (Sigma-Aldrich) for 18 h. Then, the cells were incubated in those with or without 60 ng/ml of mouse recombinant TNFα (Sigma-Aldrich) for at 37°C.

Culture of human epithelial cell line

HEC151, an endometrial epithelial cell line, was used. To induce CCA in HEC151 cells, the protocol described in the methods of culture of primary mouse uterine epithelial cells was employed.

Fluorescence assay using the cultured cells

The fluorescence assay using the cultured uterine epithelial cells was performed as described previously (Hirota *et al*, 2003). The antibodies to pMLKL (37333, Cell Signaling Technology, 1:400), MFG-E8 (D161-3, MBL, Nagoya, Japan 1:500), and pRIP3 (ab195117, Abcam, 1:200) were used.

Cell cycle analysis and annexin V assay

As for cell cycle analysis, the cells were stained with propidium iodine (Abcam), and cell fractions were quantified by flow cytometry (FACS Calibur, BD Bioscience, Bedford, MA, USA). Presentation of PS at the outer membrane of the cells was investigated using Annexin V assay kit (MBL) with flow cytometry (FACS Calibur). To evaluate annexin V-positive cells, we counted the numbers of cells on 3 randomly selected sections manually by microscopic images at × 40 magnification.

Laser capture microdissection (LCM)

LCM was performed as described previously (Haraguchi *et al*, 2014; Matsumoto *et al*, 2018). The uterine epithelium of each section was microdissected with an LMD7000 system (Leica Microsystems).

RNA-seq

RNA extracted from LCM samples was processed by SMART-seq v4 Ultra Low Input RNA Kit (Takara Bio USA, Mountain View, CA, USA) and was subjected to RNA-seq using BGI RNA-Seq service (BGI, Hong Kong, China; www.bgi.com) according to the standard protocol. The reads per kilobase of exon per million mapped sequence reads (RPKMs) were counted by FeatureCounts function in Subread (version 2.0.0) (Liao *et al*, 2013). Genes with $\log_2$ fold change (FC) > |1| were defined as differentially expressed genes (DEGs). Heatmaps of DEGs were created by Morpheus (https://software.broadinstitute.org/morpheus/). K-means clustering and visualizations of data were performed by trinityrnaseq (version 2.0.6) (Haas *et al*, 2013). Genes in each cluster were then proceeded to comparison analysis and gene ontology (GO) analysis in Enrichr (https://amp.pharm.mssm.edu/Enrichr/).

RT–qPCR

RT–qPCR was performed as described previously. Total RNA extraction from frozen whole tissues was performed as described previously (Matsumoto *et al*, 2018). A housekeeping gene (*Actb*) was used as an internal standard for normalizing the relative mRNA expression. Sequences of qPCR primers are listed in Table EV1.

Statistical analysis

Statistical analyses were performed using Fisher's exact test and a two-tailed Student *t*-test.

Data availability

The RNA-seq data from this study have been deposited to the Sequence Read Archive (SRA) (https://www.ncbi.nlm.nih.gov/Traces/study1/?acc=PRJNA658848&o=acc_s%3Aa) and assigned the identifiers (SRA: SRP278560, BioProject: PRJNA658848).

Expanded View for this article is available online.

Acknowledgements
We thank NCI mouse repository for providing *Rb1*-floxed mice, Dr. Francesco J. DeMayo (National Institute of Environmental Health Sciences, Research Triangle Park, NC, USA) and Dr. John P. Lydon (Baylor College of Medicine, Houston, TX, USA) for providing *Pgr*-Cre mice, Dr. Sudhansu K. Dey (Cincinnati Children's Hospital Medical Center, Cincinnati, OH, USA) for providing *Ltf*-Cre mice, Dr. Satoru Fukuda (The University of Tokyo, Japan) for technical assistance of TEM, Ms. Katie A. Gerhardt for efficient editing of the manuscript, and Ms. Atsumi Miura for technical assistance. This work was supported by JSPS KAKENHI (grant numbers 19H03144, 18K19601, 19H03796, 18K19600, 18H02943, 19K16022, 19K18631, 19K18630, 20K08894) and AMED-Force (20gm4010010h0001), AMED-Wise (20gk0210021h0002), Takeda Science Foundation, and the fund of joint research with NIPRO corporation.

Author contributions
Study design: SAk and YH; Experiments and data collection: SAk, YH, YF, TK, MG, THirat, THirao, MM, HH, and MS-K; Data analysis: SAk, YH, YF, and SAi; Result discussion and interpretation: RS-H, NT, TF, and YO; Manuscript writing: SAk, YH, SAi, and RS-H; Manuscript reviewing: RS-H; Study supervision: YH.

Conflict of interest
The authors declare that they have no conflict of interest.

References

Boren J, Brindle KM (2012) Apoptosis-induced mitochondrial dysfunction causes cytoplasmic lipid droplet formation. *Cell Death Differ* 19: 1561 – 1570

 © 2021 The Authors

Cha J, Sun X, Dey SK (2012) Mechanisms of implantation: strategies for successful pregnancy. *Nat Med* 18: 1754 – 1767

Chechik G, Meilijson I, Ruppin E (1999) Neuronal regulation: a mechanism for synaptic pruning during brain maturation. *Neural Comput* 11: 2061 – 2080

Chen B, Pan H, Zhu L, Deng Y, Pollard JW (2005) Progesterone inhibits the estrogen-induced phosphoinositide 3-kinase–>AKT–>GSK-3beta–>cyclin D1–>pRB pathway to block uterine epithelial cell proliferation. *Mol Endocrinol* 19: 1978 – 1990

Chen G, Deng X (2018) Cell synchronization by double thymidine block. *Bio Protoc* 8: e2994

Daikoku T, Ogawa Y, Terakawa J, Ogawa A, DeFalco T, Dey SK (2014) Lactoferrin-iCre: a new mouse line to study uterine epithelial gene function. *Endocrinology* 155: 2718 – 2724

Das SK, Wang XN, Paria BC, Damm D, Abraham JA, Klagsbrun M, Andrews GK, Dey SK (1994) Heparin-binding EGF-like growth factor gene is induced in the mouse uterus temporally by the blastocyst solely at the site of its apposition: a possible ligand for interaction with blastocyst EGF-receptor in implantation. *Development* 120: 1071 – 1083

Dey SK, Lim H, Das SK, Reese J, Paria BC, Daikoku T, Wang H (2004) Molecular cues to implantation. *Endocr Rev* 25: 341 – 373

Diaz-Gimeno P, Ruiz-Alonso M, Blesa D, Bosch N, Martinez-Conejero JA, Alama P, Garrido N, Pellicer A, Simon C (2013) The accuracy and reproducibility of the endometrial receptivity array is superior to histology as a diagnostic method for endometrial receptivity. *Fertil Steril* 99: 508 – 517

Dick FA, Rubin SM (2013) Molecular mechanisms underlying RB protein function. *Nat Rev Mol Cell Biol* 14: 297 – 306

Egashira M, Hirota Y (2013) Uterine receptivity and embryo–uterine interactions in embryo implantation: lessons from mice. *Reprod Med Biol* 12: 127 – 132

Ehrhardt H, Wachter F, Grunert M, Jeremias I (2013) Cell cycle-arrested tumor cells exhibit increased sensitivity towards TRAIL-induced apoptosis. *Cell Death Dis* 4: e661

Franco HL, Rubel CA, Large MJ, Wetendorf M, Fernandez-Valdivia R, Jeong JW, Spencer TE, Behringer RR, Lydon JP, Demayo FJ (2012) Epithelial progesterone receptor exhibits pleiotropic roles in uterine development and function. *FASEB J* 26: 1218 – 1227

Fukui Y, Hirota Y, Matsuo M, Gebril M, Akaeda S, Hiraoka T, Osuga Y (2019) Uterine receptivity, embryo attachment, and embryo invasion: multistep processes in embryo implantation. *Reprod Med Biol* 18: 234 – 240

Giacinti C, Giordano A (2006) RB and cell cycle progression. *Oncogene* 25: 5220 – 5227

Guo Y, Cordes KR, Farese Jr RV, Walther TC (2009) Lipid droplets at a glance. *J Cell Sci* 122: 749 – 752

Haas BJ, Papanicolaou A, Yassour M, Grabherr M, Blood PD, Bowden J, Couger MB, Eccles D, Li B, Lieber M *et al* (2013) De novo transcript sequence reconstruction from RNA-seq using the Trinity platform for reference generation and analysis. *Nat Protoc* 8: 1494 – 1512

Hanayama R, Tanaka M, Miwa K, Shinohara A, Iwamatsu A, Nagata S (2002) Identification of a factor that links apoptotic cells to phagocytes. *Nature* 417: 182 – 187

Haraguchi H, Saito-Fujita T, Hirota Y, Egashira M, Matsumoto L, Matsuo M, Hiraoka T, Koga K, Yamauchi N, Fukayama M *et al* (2014) MicroRNA-200a locally attenuates progesterone signaling in the cervix, preventing embryo implantation. *Mol Endocrinol* 28: 1108 – 1117

Haraguchi H, Hirota Y, Saito-Fujita T, Tanaka T, Shimizu-Hirota R, Harada M, Akaeda S, Hiraoka T, Matsuo M, Matsumoto L *et al* (2019) Mdm2-p53-SF1 pathway in ovarian granulosa cells directs ovulation and fertilization by conditioning oocyte quality. *FASEB J* 33: 2610 – 2620

Harper JV (2005) Synchronization of cell populations in G1/S and G2/M phases of the cell cycle. *Methods Mol Biol* 296: 157 – 166

Hirota Y, Osuga Y, Yoshino O, Koga K, Yano T, Hirata T, Nose E, Ayabe T, Namba A, Tsutsumi O *et al* (2003) Possible roles of thrombin-induced activation of protease-activated receptor 1 in human luteinized granulosa cells. *J Clin Endocrinol Metab* 88: 3952 – 3957

Hirota Y, Daikoku T, Tranguch S, Xie H, Bradshaw HB, Dey SK (2010) Uterine-specific p53 deficiency confers premature uterine senescence and promotes preterm birth in mice. *J Clin Invest* 120: 803 – 815

Hirota Y (2019) Progesterone governs endometrial proliferation-differentiation switching and blastocyst implantation. *Endocr J* 66: 199 – 206

Huet YM, Dey SK (1987) Role of early and late oestrogenic effects on implantation in the mouse. *J Reprod Fertil* 81: 453 – 458

Inhorn MC, Patrizio P (2015) Infertility around the globe: new thinking on gender, reproductive technologies and global movements in the 21st century. *Hum Reprod Update* 21: 411 – 426

Joswig A, Gabriel HD, Kibschull M, Winterhager E (2003) Apoptosis in uterine epithelium and decidua in response to implantation: evidence for two different pathways. *Reprod Biol Endocrinol* 1: 44

Li Q, Kannan A, DeMayo FJ, Lydon JP, Cooke PS, Yamagishi H, Srivastava D, Bagchi MK, Bagchi IC (2011) The antiproliferative action of progesterone in uterine epithelium is mediated by Hand2. *Science* 331: 912 – 916

Li Y, Sun X, Dey SK (2015) Entosis allows timely elimination of the luminal epithelial barrier for embryo implantation. *Cell Rep* 11: 358 – 365

Liao Y, Smyth GK, Shi W (2013) The Subread aligner: fast, accurate and scalable read mapping by seed-and-vote. *Nucleic Acids Res* 41: e108

Lydon JP, DeMayo FJ, Funk CR, Mani SK, Hughes AR, Montgomery Jr CA, Shyamala G, Conneely OM, O'Malley BW (1995) Mice lacking progesterone receptor exhibit pleiotropic reproductive abnormalities. *Genes Dev* 9: 2266 – 2278

Ma WG, Song H, Das SK, Paria BC, Dey SK (2003) Estrogen is a critical determinant that specifies the duration of the window of uterine receptivity for implantation. *Proc Natl Acad Sci USA* 100: 2963 – 2968

Marino S, Vooijs M, van Der Gulden H, Jonkers J, Berns A (2000) Induction of medulloblastomas in p53-null mutant mice by somatic inactivation of Rb in the external granular layer cells of the cerebellum. *Genes Dev* 14: 994 – 1004

Matsumoto H, Ma WG, Daikoku T, Zhao X, Paria BC, Das SK, Trzaskos JM, Dey SK (2002) Cyclooxygenase-2 differentially directs uterine angiogenesis during implantation in mice. *J Biol Chem* 277: 29260 – 29267

Matsumoto L, Hirota Y, Saito-Fujita T, Takeda N, Tanaka T, Hiraoka T, Akaeda S, Fujita H, Shimizu-Hirota R, Igaue S *et al* (2018) HIF2α in the uterine stroma permits embryo invasion and luminal epithelium detachment. *J Clin Invest* 128: 3186 – 3197

Matsuo M, Hirota Y, Fukui Y, Fujita H, Saito-Fujita T, Kaku T, Gebril M, Hirata T, Akaeda S, Hiraoka T *et al* (2020) Levonorgestrel inhibits embryo attachment by eliminating uterine induction of leukemia inhibitory factor. *Endocrinology* 161: bqz005

Overholtzer M, Mailleux AA, Mouneimne G, Normand G, Schnitt SJ, King RW, Cibas ES, Brugge JS (2007) A nonapoptotic cell death process, entosis, that occurs by cell-in-cell invasion. *Cell* 131: 966 – 979

Schlafke S, Enders AC (1975) Cellular basis of interaction between trophoblast and uterus at implantation. *Biol Reprod* 12: 41 – 65

© 2021 The Authors

Schwarting R, Gerdes J, Niehus J, Jaeschke L, Stein H (1986) Determination of the growth fraction in cell suspensions by flow cytometry using the monoclonal antibody Ki-67. *J Immunol Methods* 90: 65 – 70

Segawa K, Yanagihashi Y, Yamada K, Suzuki C, Uchiyama Y, Nagata S (2018) Phospholipid flippases enable precursor B cells to flee engulfment by macrophages. *Proc Natl Acad Sci USA* 115: 12212 – 12217

Shlomovitz I, Speir M, Gerlic M (2019) Flipping the dogma – phosphatidylserine in non-apoptotic cell death. *Cell Commun Signal* 17: 139

Soyal SM, Mukherjee A, Lee KY, Li J, Li H, DeMayo FJ, Lydon JP (2005) Cre-mediated recombination in cell lineages that express the progesterone receptor. *Genesis* 41: 58 – 66

Tang D, Kang R, Berghe TV, Vandenabeele P, Kroemer G (2019) The molecular machinery of regulated cell death. *Cell Res* 29: 347 – 364

Tong W, Pollard JW (1999) Progesterone inhibits estrogen-induced cyclin D1 and cdk4 nuclear translocation, cyclin E- and cyclin A-cdk2 kinase activation, and cell proliferation in uterine epithelial cells in mice. *Mol Cell Biol* 19: 2251 – 2264

Tranguch S, Wang H, Daikoku T, Xie H, Smith DF, Dey SK (2007) FKBP52 deficiency-conferred uterine progesterone resistance is genetic background and pregnancy stage specific. *J Clin Invest* 117: 1824 – 1834

Vasquez YM, Wang X, Wetendorf M, Franco HL, Mo Q, Wang T, Lanz RB, Young SL, Lessey BA, Spencer TE *et al* (2018) FOXO1 regulates uterine epithelial integrity and progesterone receptor expression critical for embryo implantation. *PLoS Genet* 14: e1007787

Wetendorf M, Wu S-P, Wang X, Creighton CJ, Wang T, Lanz RB, Blok L, Tsai SY, Tsai M-J, Lydon JP *et al* (2017) Decreased epithelial progesterone receptor A at the window of receptivity is required for preparation of the endometrium for embryo attachment†. *Biol Reprod* 96: 313 – 326

Yamanaka K, Urano Y, Takabe W, Saito Y, Noguchi N (2014) Induction of apoptosis and necroptosis by 24(S)-hydroxycholesterol is dependent on activity of acyl-CoA:cholesterol acyltransferase 1. *Cell Death Dis* 5: e990

Yoshinaga K, Adams CE (1966) Delayed implantation in the spayed, progesterone treated adult mouse. *J Reprod Fertil* 12: 593 – 595

Zargarian S, Shlomovitz I, Erlich Z, Hourizadeh A, Ofir-Birin Y, Croker BA, Regev-Rudzki N, Edry-Botzer L, Gerlic M (2017) Phosphatidylserine externalization, "necroptotic bodies" release, and phagocytosis during necroptosis. *PLoS Biol* 15: e2002711

Zhu Y, Cui H, Xia Y, Gan H (2016) RIPK3-mediated necroptosis and apoptosis contributes to renal tubular cell progressive loss and chronic kidney disease progression in rats. *PLoS One* 11: e0156729

 © 2021 The Authors